

1 **Mg/Ca, Sr/Ca AND STABLE ISOTOPES FROM THE PLANKTONIC**
2 **FORAMINIFERA *T. SACCULIFER*: TESTING A MULTI-PROXY APPROACH FOR**
3 **INFERRING PALEO-TEMPERATURE AND PALEO-SALINITY**
4
5

6 Delphine Dissard (1, 2), Gert Jan Reichart (3, 4), Christophe Menkes (5), Morgan Mangeas (5), Stephan
7 Frickenhaus (2) and Jelle Bijma (2)

8
9 (1) UMR LOCEAN (IRD-CNRS-MNHN-Sorbonne Université), Centre IRD de Nouméa 101 Promenade Roger Laroque,
10 Noumea 98848, New Caledonia.

11 (2) Alfred-Wegener-Institute, Helmholtz-Zentrum für Polar- und Meeres Forschung, Am Handelshafen 12, 27570
12 Bremerhaven, Germany

13 (3) NIOZ Royal Natherlands Inst. Sea Res, Den Burg, Texel, Netherlands.

14 (4) Univ. Utrecht, Fac Geosci. Dept Earth Sci. Utrecht, Netherlands

15 (5) UMR ENTROPIE (IRD, Univ. de la Réunion, CNRS, IFREMER, UNC), Centre IRD de Nouméa 101 Promenade Roger
16 Laroque, Noumea 98848, New Caledonia.
17

18
19
20
21
22 **ABSTRACT**
23

24 Over the last decades, sea surface temperature (SST) reconstructions based on the Mg/Ca of
25 foraminiferal calcite have frequently been used in combination with the $\delta^{18}\text{O}$ signal from the
26 same material, to provide estimates of $\delta^{18}\text{O}$ of the water ($\delta^{18}\text{O}_w$), a proxy for global ice volume
27 and sea surface salinity (SSS). However, because of error propagation from one step to the next,
28 better calibrations are required to increase accuracy and robustness of existing isotope and
29 element to temperature proxy-relationships. Towards that goal, we determined Mg/Ca, Sr/Ca
30 and the oxygen isotopic composition of *Trilobatus sacculifer* (previously referenced as
31 *Globigerinoides sacculifer*), collected from surface waters (0-10m), along a North-South
32 transect in the eastern basin of the tropical/subtropical Atlantic Ocean. We established a new
33 paleo-temperature calibration based on Mg/Ca, and on the combination of Mg/Ca and Sr/Ca.
34 Subsequently, a sensitivity analysis was performed in which, one, two, or three different
35 equations were considered. Results indicate that foraminiferal Mg/Ca allow for an accurate
36 reconstruction of surface water temperature. Combining equations, $\delta^{18}\text{O}_w$ can be reconstructed
37 with a precision of about $\pm 0.5\%$. However, the best possible salinity reconstruction based on
38 locally calibrated equations, only allowed reconstruction with an uncertainty of ± 2.49 . This was
39 confirmed by a Monte Carlo simulation, applied to test successive reconstructions in an ‘ideal
40 case’, where explanatory variables are known. This simulation shows that from a pure statistical
41 point of view, successive reconstructions involving Mg/Ca and $\delta^{18}\text{O}_c$ preclude salinity

42 reconstruction with a precision better than ± 1.69 and hardly better than ± 2.65 , due to error
43 propagation. Nevertheless, a direct linear fit to reconstruct salinity based on the same measured
44 variables (Mg/Ca and $\delta^{18}O_c$) was established. This direct reconstruction of salinity lead to a
45 much better estimation of salinity (± 0.26) than the successive reconstructions.

46

47

48

I. INTRODUCTION

49

50 Since Emiliani's pioneering work (1954), oxygen isotope compositions recorded in fossil
51 foraminiferal shells became a major tool to reconstruct past sea surface temperature. After
52 Shackleton's seminal studies (1967, 1968 and 1974), it became clear that part of the signal
53 reflected glacial-interglacial changes in continental ice volume and hence sea level variations.
54 The oxygen isotope composition of foraminiferal calcite ($\delta^{18}O_c$) is thus controlled by the
55 temperature of calcification (Urey, 1947; Epstein et al., 1953) but also by the oxygen isotope
56 composition of seawater ($\delta^{18}O_w$). The relative contribution of these two factors cannot be
57 deconvolved without an independent measure of the temperature at the time of calcification
58 such as e.g. Mg/Ca (e.g. Nürnberg et al., 1996; Rosenthal et al., 1997; Rathburn and DeDeckker,
59 1997; Hastings et al., 1998; Lea et al., 1999; Lear et al., 2002; Toyofuku et al., 2000; Anand et
60 al., 2003, al., Kisakurek et al., 2008; Duenas-Bohorquez et al., 2009, 2011; Honisch et al., 2013;
61 Kontakiotis et al., 2016; Jentzen et al., 2018). The sea surface temperature (SST) reconstructed
62 from Mg/Ca of foraminiferal calcite has, therefore, increasingly been used in combination with
63 the $\delta^{18}O$ signal measured on the same material, to estimate $\delta^{18}O_w$, global ice volume and to
64 infer past sea surface salinity (SSS) (e.g. Rohling 2000, Elderfield and Ganssen, 2000; Schmidt
65 et al., 2004; Weldeab et al., 2005; 2007). These studies also showed that, because of error
66 propagation, inaccuracies in the different proxies combined for the reconstruction of past sea
67 water $\delta^{18}O$ and salinity obstruct meaningful interpretations. Hence, while there is an
68 understandable desire to apply empirical proxy-relationships down-core, additional calibrations
69 appear necessary to make reconstructions more robust. Calibrations using foraminifera sampled
70 from surface seawater (0-10m deep), provide the best possibility to avoid most of the artefacts
71 usually seen when using specimen from core tops or culture experiments for calibration
72 purposes. Here, we report a calibration based on *Globigerinoides sacculifer*, which should now
73 and will be referenced in this manuscript as *Trilobatus sacculifer* (Spezzaferrri et al., 2015),
74 from the Atlantic Ocean. Mg and Sr concentrations were measured on the last chamber of
75 individual specimens with Laser Ablation-Inductively Coupled Plasma-Mass Spectrometry

76 (LA-ICP-MS), while the oxygen isotope composition of the same tests as used for the elemental
77 analyses was subsequently measured by Isotope ratio Mass Spectrometry (IRMS).
78 Environmental parameters (temperature: T, salinity: S, dissolved inorganic carbon: DIC and
79 alkalinity: ALK) but also the isotopic composition (O^{18}_w) of the seawater the foraminifera were
80 growing in, were measured. The primary objectives of this study are (1) to test and improve the
81 calibration of both the Mg/Ca and oxygen isotope paleothermometer for the paleoceanographic
82 relevant species *T. sacculifer*; (2) to test whether the incorporation of Sr into the Mg-T
83 reconstruction equation improves temperature reconstruction by accounting for the impact of
84 salinity; (3) evaluate the agreement between observed and predicted $\delta^{18}O_w$ and (4) test potential
85 for SSS reconstructions of the Atlantic Ocean. Our results indicate that the best possible salinity
86 reconstruction based on locally calibrated equations from the present study, only allowed
87 reconstruction with an uncertainty of ± 2.49 . Such an uncertainty does not allow for viable
88 (paleo)salinity data. This is subsequently confirmed by a Monte Carlo simulation, applied to
89 test successive reconstructions in an ‘ideal case’, where explanatory variables are known. This
90 simulation shows that from a pure statistical point of view, successive reconstructions involving
91 Mg/Ca and $\delta^{18}O_c$ preclude salinity reconstruction with a precision better than ± 1.69 and hardly
92 better than ± 2.65 , due to error propagation. Nevertheless, a direct linear fit based on the same
93 measured variables (Mg/Ca and $\delta^{18}O_c$), and leading to much better estimation of salinity
94 (± 0.26), could be established.

95

96

2. MATERIAL AND METHODS

97

2.1. Collection procedure

98 Foraminifera were collected between October and November 2005, on board of the research
99 vessel Polarstern (ANT XXIII/1) during a meridional transect of the Atlantic Ocean
100 (Bremerhaven/Germany - Cape Town/South of Africa; Fig. 1a). Foraminifera were
101 continuously collected from a depth of ca. 10 m using the ship’s membrane pump (3 m³/h). The
102 water flowed into a plankton net (125 μ m) that was fixed in a 1000 L plastic tank with an
103 overflow (Fig 1b). Every eight hours, the plankton accumulated in the net was collected.
104 Temperature and salinity of surface seawaters were continuously recorded by the ship’s
105 systems, and discrete water samples were collected for later analyses of total ALK, DIC and
106 $\delta^{18}O_w$ (see Tab. 1). Plankton and water samples were poisoned with buffered formaldehyde
107 solution (20%) and HgCl₂ (1.5 ml with 70gL⁻¹ HgCl₂ for 1 L samples), respectively. In total,
108 more than seventy plankton samples were collected during the transect, covering a large range
109

110 in both temperature and salinity. Specimens of *T. sacculifer* from thirteen selected stations,
111 selected as to maximize temperature and salinity ranges, were picked and prepared for analyses.
112 Salinity, temperature, DIC, ALK and $\delta^{18}\text{O}_w$ data reported in this paper represent
113 October/November values for the selected stations.

114

115 **2.2. Description of species**

116 *Trilobatus sacculifer* is a spinose species with endosymbiotic dinoflagellates inhabiting the
117 shallow (0-80 m deep) tropical and subtropical regions of the world oceans. This species
118 displays a large tolerance to temperature (14-32°C) and salinity (24-47) (Hemleben et al., 1989;
119 Bijma et al., 1990). Based on differences in the shape of the last chamber of adult specimens,
120 various morphotypes can be distinguished. Among others the last chamber can be smaller than
121 the penultimate chamber, in which case it is called kummerform (kf). This species shows an
122 ontogenetic depth migration and predominantly reproduces at depth around full moon (Bijma
123 and Hemleben, 1993). Just prior to reproduction a secondary calcite layer, called gametogenic
124 (GAM) calcite is added (Bé et al., 1982; Bijma and Hemleben, 1993; Bijma et al., 1994).
125 Juveniles (<100 μm) ascend in the water column and reach the surface after less than
126 approximately 2 weeks. Pre-adult stages then slowly descend within 9-10 days to the
127 reproductive depth. In our samples (collected between 0 and 10 m depth), *T. sacculifer*
128 specimens have not yet added the Mg-enriched gametogenic calcite, which generally occurs
129 deeper in the water column just prior to reproduction. Therefore, only the trilobus morphotype
130 without GAM calcite is considered in this study, which limits the environmental, ontogenetic
131 and physiological variability between samples even if a rather wide size fraction (230 to
132 500 μm) was selected due to sample size limitation. This should be taken into account when
133 compared to other calibrations based on core top and/or sediment trap collected specimen

134

135 **2.3. Seawater analysis**

136 The DIC and ALK analyses of the sea water were carried out at the Leibniz Institute of Marine
137 Sciences at the Christian-Albrechts University of Kiel, (IFM-GEOMAR), Germany. Analyses
138 were performed by extraction and subsequent coulometric titration of evolved CO_2 for DIC
139 (Johnson et al., 1993), and by open-cell potentiometric seawater titration for ALK (Mintrop et
140 al., 2000). Precision / accuracy of DIC and ALK measurements are 1 $\mu\text{mol kg}^{-1}$ / 2 $\mu\text{mol kg}^{-1}$
141 and 1.5 $\mu\text{mol kg}^{-1}$ / 3 $\mu\text{mol kg}^{-1}$, respectively. Accuracy of both DIC and ALK was assured by
142 the analyses of certified reference material (CRM) provided by Andrew Dickson from Scripps
143 Institution of Oceanography, La Jolla, USA. Measurements of $\delta^{18}\text{O}_w$ were carried out at the

144 Faculty of Geosciences, Utrecht University, Netherlands. Samples were measured using a
145 GasBench II - Delta plus XP combination. Results were corrected for drift with an in-house
146 standard (RMW) and are reported on V-SMOW scale, with a precision of 0.1‰ and accuracy
147 verified against NBS 19 of 0.2‰ respectively. For reconstruction calculations $\delta^{18}\text{O}$ data were
148 corrected to the PDB scale by subtracting 0.27‰ (Hut, 1987).

149

150 **2.4. Carbonate analysis**

151 2.4.1. Foraminiferal sample preparation

152 Under a binocular microscope, maximum test diameter of each specimen was measured and
153 individual tests were weighed on a microbalance (METTLER TOLEDO, precision $\pm 0.1\mu\text{g}$).
154 Since the foraminifera were never in contact with sediments, the rigorous cleaning procedure
155 required for specimens collected from sediment cores, was not necessary. Prior to analysis the
156 tests were cleaned following a simplified cleaning procedure: All specimens were soaked for
157 30 min in a 3-7% NaOCl solution (Gaffey and Brönniman, 1993). A stereomicroscope was used
158 during cleaning and specimens were removed from the reagent directly after complete
159 bleaching. The samples were immediately and thoroughly rinsed with deionised water to ensure
160 complete removal of the reagent. After cleaning, specimens were inspected with scanning
161 electron microscopy and showed no visible signs of dissolution. This cleaning procedure
162 preserves original shell thickness and thus maximises data acquisition during laser ablation.
163 Foraminifera were fixed on a double-sided adhesive tape and mounted on plastic stubs for LA-
164 ICP-MS analyses.

165

166 2.4.2. Elemental composition analysis

167 For each station, 5–13 specimens were analysed. Their last chambers were ablated using an
168 Excimer 193 nm deep ultraviolet laser (Lambda Physik) with GeoLas 200Q optics (Reichert et
169 al, 2003) creating 80 μm diameter craters. Pulse repetition rate was set at 6 Hz, with an energy
170 density at the sample surface of 1 J/cm^2 . The ablated material was transported on a continuous
171 helium flow into the argon plasma of a quadrupole ICP-MS instrument (Micromass Platform)
172 and analysed with respect to time. Ablation of calcite requires ultraviolet wavelengths as an
173 uncontrolled disruption would result from higher wavelengths. By using a collision and reaction
174 cell spectral interferences on the minor isotopes of Ca (^{42}Ca , ^{43}Ca and ^{44}Ca) were reduced and
175 interferences of clusters like $^{12}\text{C}^{16}\text{O}^{16}\text{O}$ were prevented. Analyses were calibrated against NIST
176 (U.S. National Institute of Standards and Technology) 610 glass using the concentration data
177 of Jochum et al. (2011) with Ca as internal standard. For Ca quantification, mass 44 was used

178 while monitoring masses 42 and 43 as internal check. In the calcite, the Ca concentration was
179 set at 40%, allowing direct comparison to trace metal/Ca from traditional wet-chemical studies.
180 Mg concentrations were calculated using masses 24 and 26; Sr concentrations were calculated
181 with mass 88. One big advantage in using LA-ICP-MS measurements is that single laser pulses
182 remove only a few nanometers of material, which allows high resolution trace elements profiles
183 to be acquired (e.g. Reichart et al., 2003; Regenberg et al., 2006; Dueñas-Bohórquez et al.,
184 2009, 2010, Hathorne et al., 2009; Munsel et al., 2010; Dissard et al., 2009; 2010a and b; Evans
185 et al., 2013; 2015; Steinhardt 2014, 2015; Fehrenbacher et al., 2015; Langer et al., 2016; Koho
186 et al., 2015; 2017; Fontanier et al., 2017; De Nooijer et al., 2007, 2014, 2017a and b; Jentzen et
187 al., 2018, Schmitt et al., 2019; Levi et al., 2019). Element concentrations were calculated for
188 the individual ablation profiles integrating the different isotopes (glitter software). Even though
189 the use of a single or very few specimens, can be criticised when determining foraminifera
190 Mg/Ca and $\delta^{18}\text{O}$ in order to perform paleoclimate reconstructions instead of more traditional
191 measurements, Groeneveld et al., (2019) recently demonstrated that for both proxies, single
192 specimen variability is dominated by seawater temperatures during calcification, even if the
193 presence of an ecological effect leading to site-specific seasonal and depth habitat changes is
194 also noticeable.

195

196 **2.5. Stable isotope analysis**

197 The specimens used for elemental composition analyses using LA-ICP-MS were subsequently
198 carefully removed from the plastic stubs and rinsed with deionised water before measuring their
199 stable isotope composition. Depending on shell weight, 2 to 3 foraminifera were necessary to
200 obtain a minimum of 20 μg of material, required for each analysis. Analyses were carried out in
201 duplicate for each station. The results, compiled in table 2, represent average measurements.
202 The analyses were carried out at the Department of Earth Sciences of Utrecht University (The
203 Netherlands), using a Kiel-III -Finnigan MAT-253 mass spectrometer combination. The $\delta^{18}\text{O}_\text{c}$
204 results are reported in ‰ PDB. Calibration was made with NBS-19 (precision of 0.06-0.08 ‰
205 for sample size 20-100 μg , accuracy better than 0.2‰).

206

207 **2.6. Statistical analysis**

208 Within this manuscript, all statistical analyses with regards to elemental and isotopic data, were
209 carried out using the program R with default values (R Development Core Team (2019)).

210

211

3. RESULTS

212

213 3.1. Elemental composition

214 Overall values of the Mg/Ca and Sr/Ca ratios in the tests of *T. sacculifer* varied from 1.78 to
215 5.86 mmol/mol (Fig. 2a) and 1.41 to 1.52 mmol/mol (fig. 2b), respectively (Tab. 2). These
216 Mg/Ca concentrations compare well with results found in literature for this species from either
217 culture experiments, plankton tow, or surface sediment, growing at the same temperatures (e.g.
218 Nürnberg et al., 1996; Anand et al. 2003, Regenberg et al., 2009, Fig. 3). Similarly, the overall
219 variation in Sr/Ca-values reported in this study is comparable to that observed in core top and
220 cultured *G. ruber* and *T. sacculifer* combined, for comparable salinity and temperature
221 conditions, (varying between 1.27 to 1.51mmol/mol; e.g. Cleroux et al., 2008; Kısakürek et al.,
222 2008; Dueñas-Bohórquez et al., 2009).

223

224 The relationship between both Mg/Ca and Sr/Ca ratios and measured temperatures were
225 calculated using least square differences. Both show a good correlation with surface water
226 temperature (Fig. 2, Tab. 3). The Mg/Ca ratio increases exponentially by 8.3%/°C (best fit)
227 (Mg/Ca and Sr/Ca ratios given in mmol/mol):

$$228 \text{Mg/Ca}=(0.42\pm 0.13) \exp((0.083\pm 0.001)*T), R^2=0.86 \quad \text{pvalue}=2,9\text{e-}06 \quad (\text{equation 1})$$

229

230 whereas Sr/Ca ratio increases linearly by 0.6%/°C (Fig. 2a and b), best fit:

$$231 \text{Sr/Ca}=(0.009\pm 0.002)*T+(1.24\pm 0.05), R^2=0.67 \quad \text{pvalue}=5.\text{e-}04 \quad (\text{equation 2})$$

233

234 Concerning the temperature reconstruction, by inverting the approach, univariate regressions
235 yields to:

$$236 T=(12.3\pm 1.5)+((10.5\pm 1.2)*\log(\text{Mg/Ca}), R^2=0.86 \quad \text{pvalue}=2,9\text{e-}06 \quad (\text{equation 1'})$$

237 And

$$238 T=+(-84.1\pm 22.9)+((71.7\pm 15)*\text{Sr/Ca}), R^2=0.67 \quad \text{pvalue}=5\text{e-}04 \quad (\text{equation 2'})$$

239

240 Combining Mg and Sr data for a non-linear multivariate regression allows improvement of the
241 correlation with temperature, best fit:

242

$$243 T=- (27\pm 15)+ (8\pm 1)*\ln(\text{Mg/Ca})+(28\pm 11)*\text{Sr/Ca}, \text{pvalue Mg/Ca: } 2.10^{-4} \quad (\text{equation 3})$$

244

$$R^2=0.92 \quad \text{pvalue}= 2.\text{e-}04$$

245 For comparison, with regression found in the literature, Mg/Ca is estimated below as a function
246 of temperature and Sr/Ca:

$$247 \quad \text{Mg/Ca} = \exp((0.98 \pm 1.89) + (0.09 \pm 0.02) * T + (-1.43 \pm 1.45) * \text{Sr/Ca})$$
$$248 \quad R^2 = 0.86 \quad \text{pvalue} = 2.05e-05 \quad (\text{equation 3'})$$

249
250 Regression for the relationship between salinity and Mg/Ca ratios does not show any clear
251 correlation ($R^2=0.09$, $p\text{-value}=0.32$). This is in good agreement with previous culture
252 experiments studies which only report a minor sensitivity of Mg/Ca to salinity in planktonic
253 foraminifera (e.g. Dueñas-Bohórquez et al., 2009; Hönisch et al., 2013; Kisakürek et al., 2008;
254 Nürnberg et al., 1996). The correlation observed between Sr/Ca ratios and salinity ($R^2=0.29$, $p\text{-}$
255 $\text{value}=0.053$) is better compared to that between Mg/Ca and salinity, but remains relatively
256 weak. Nevertheless, recalculated regressions of Mg/Ca, incorporating salinity, show an
257 improvement of the correlation with temperature, best fit:

$$258$$
$$259 \quad \text{Mg/Ca} = \exp((-5.02 \pm 2) + (0.09 \pm 0.009) * T + (0.11 \pm 0.05) * S),$$
$$260 \quad R^2 = 0.91 \quad \text{pvalue} = 5e-06$$

261
262 This result is in good agreement with the recent study of Gray and Evans (2019), who reported
263 the minor Mg/Ca sensitivity of *Trilobatus sacculifer* to salinity ($3.6 \pm 0.01\%$ increase per
264 salinity unit) and described, based on previously published culture experiments' data (Dueñas-
265 Bohórquez et al., 2009; Hönisch et al., 2013; Kisakürek et al., 2008; Lea et al., 1999; Nürnberg
266 et al., 1996), a similar fit allowing to assess the sensitivity of foraminiferal Mg/Ca of *T.*
267 *sacculifer* to temperature and salinity combined.

$$268 \quad \text{Mg/Ca} = \exp(0.054(S-35) + 0.062T - 0.24) \quad \text{RSE: } 0.51 \quad \text{Gray and Evans (2019)}$$

269 Applying the equation of Gray and Evans (2019), to our data, leads to a correlation of 0.90,
270 which is identical than our findings. In order to further compare both equations, Mg/Ca values
271 from our study were used to reconstruct temperature and salinity using the fit established per
272 Gray and Evans (2019), versus reconstructed temperature and salinity using our fit. The
273 observed R^2 are then 0.99 and 0.48 for temperature and salinity, respectively. We can conclude,
274 that if the equation of Gray and Evans (2019), is in perfect agreement with our equation with
275 regards to the temperature parameter, this is not the case for salinity, which shows a strong
276 difference between the two equations, most probably explained by the weak correlation of
277 Mg/Ca to salinity in our data. Subsequently, the Bayesian model of Tierney et al. (2019)

278 considering the group-specific core-top model for *T. sacculifer* was applied to our data. In that
279 aim, Ω^{-2} and pH, were calculated using Alk and DIC data presented in table 1. Because
280 foraminifera in our studies were not submitted to cleaning protocol with a reductive step, the
281 clean parameter was set to 0. It led to the following correlation:

$$282 \quad \text{Mg/Ca} = \exp(-11.66 + 0.06 * T - 0.21 \Omega^{-2} + 1.40 \text{pH}) \quad R^2 = 0.82$$

283 Here we can conclude, that despite the difference in sampling strategy and samples
284 geographical distribution, our regression models are in line with the previous work of Gray and
285 Evans (2019) and Tierney et al. (2019).

286 **3.2. Stable isotopes concentration**

287 The $\delta^{18}\text{O}$ (PDB) values of the tests ($\delta^{18}\text{Oc}$) and of the seawater ($\delta^{18}\text{Ow}$) vary from -0.70 to -
288 2.98‰ and from 0.74 to 1.25‰, respectively (Tab. 1 and 2). The relationship between
289 temperature and the foraminiferal $\delta^{18}\text{O}$ (expressed as a difference to the $\delta^{18}\text{Ow}$ of the ambient
290 seawater) was estimated with a linear least squares regression:

$$291 \quad T = (11.82 \pm 1.3) - (4.82 \pm 0.45) * (\delta^{18}\text{Oc} - \delta^{18}\text{Ow}) [\text{‰}]; R^2 = 0.90 \quad (\text{equation 4})$$

292
293
294 The oxygen isotope fractionation ($\delta^{18}\text{Oc} - \delta^{18}\text{Ow}$) shows a strong correlation with *in situ* surface
295 water temperature (linear increase of 0.17‰/°C).

296 297 **3.3. Comparison with previously established *T. sacculifer* temperature reconstruction** 298 **equations**

299 As mentioned above, average juvenile and pre-adult *T. sacculifer* specimen only spend between
300 9 to 10 days in surface waters. Therefore, measured *in situ* temperature is representative of the
301 calcification temperatures. This is supported by the strong correlation between measured
302 temperature and $\delta^{18}\text{O}$ analyses ($R^2=0.90$, equation 4), and measured temperature vs. Mg/Ca,
303 ($R^2=0.87$, equation 1). Nevertheless, diurnal variations in temperatures cannot be discarded and
304 may induce a slight offset between measured average temperature and mean calcification
305 temperature.

306
307 For comparison, three Mg/Ca temperature calibrations for *T. sacculifer* were considered in this
308 manuscript. The equation of Nürnberg et al. (1996) based on laboratory cultures, (2) the
309 equation established by Anand et al. (2003) based on sediment trap samples and (3) the equation

310 derived by Regenberg et al. (2009) based on surface sediment samples of the Tropical Atlantic
311 Ocean. In each of these studies only *T. sacculifer* without SAC chamber were considered, (Tab.
312 3).

313 Similarly, in addition to equation 4 established in this study, three $\delta^{18}\text{O}$ based paleo-temperature
314 equations for *T. sacculifer* were used for comparison with our data set: (1) Erez and Luz, (1983)
315 and, (2) Spero et al. (2003), both based on cultured specimens, and (3) Mulitza et al. (2003)
316 based on surface water samples (Fig. 4; Tab. 3).

317

318 **3.4. Correlation between measured $\delta^{18}\text{O}$ /Salinity**

319 Salinity and the oxygen isotope composition of surface seawater were measured for 23 stations
320 located between 33°N and 27°S of the Eastern Atlantic Ocean (Tab. 4), including the thirteen
321 stations represented in figure 1, where foraminifera were sampled. The $\delta^{18}\text{O}_w$ -salinity
322 relationship (equation 5) is plotted in figure 5.

323

$$324 \quad \delta^{18}\text{O}_w = (0.194 \pm 0.04) * S - (5.8 \pm 1.5), R^2 = 0.53 \quad (\text{equation 5})$$

325

326 For comparison, the $\delta^{18}\text{O}_w$ -salinity relationship for the tropical Atlantic Ocean calculated by
327 Paul et al. (1999) (from 25°S to 25°N) based on GEOSECS data, and by Regenberg et al.
328 (2009), based on data from Schmidt 1999 (30°N–30°S), are plotted in the same figure.
329 Temporal, geographical and depth differences in sampling, as well as analytical noise, are most
330 probably responsible for the observed variations.

331

332

4. DISCUSSION

333 **4.1. Intra-test variability**

334 The Mg/Ca and Sr/Ca composition of foraminiferal calcium carbonate was determined using
335 laser ablation ICP-MS of the final (F) chamber of size-selected specimen. Eggins et al., (2003)
336 report that the Mg/Ca composition of sequentially precipitated chambers of different species
337 (including *T. sacculifer*) are consistent with temperature changes following habitat migration
338 towards adult life-cycle stages. As described for *T. sacculifer* in the Red Sea (Bijma and
339 Hemleben, 1994), juvenile specimens (<100 μm) migrate to the surface, where they stay about
340 9-10 days, before descending to the reproductive depth (80m). The addition of GAM calcite
341 proceeds immediately prior to gamete release (Hamilton et al., 2008). The specimens
342 considered in this study were collected between 0 and 10 meters depth, and in agreement with
343 measurements on specimens from culture experiments (Dueñas-Bohórquez, 2009), Mg-rich

344 external surfaces (GAM calcite) were not observed in our samples. This indicates limited
345 vertical migration (see section 2.2. for reproduction cycle), reducing therewith potential
346 ontogenic vital effects responsible for inter-chamber elemental variations (Dueñas-Bohórquez,
347 2010) and, limited, if any, GAM calcite precipitation (Nürnberg et al., 1996). If the exact
348 calcification depth of the last chambers of our *T. sacculifer* specimen can still be questioned,
349 the lack of GAM-calcite, together with the strong correlation observed between measured
350 surface temperature vs. Mg/Ca-reconstructed temperature, support the idea that calcification of
351 the last chamber of our specimen occurred around 10 meters depth. It should be noted that Lessa
352 et al. (2020) recently confirmed that *T. sacculifer* calcifies in the upper 30 m. Because the
353 diameter of the laser beam used in this study was 80 μ m, it represents a reliable mean value of
354 elemental concentration of the last chamber wall, for every analysis of a single shell a full
355 ablation of the wall chamber was performed (until perforation was completed). For comparison,
356 results from traditional ICP-OES Mg/Ca analyses (Regenberg et al., 2009), electron microprobe
357 (Nurnberg et al., 1996) and laser ablation ICP-MS (this study) are plotted in figure 3a and
358 suggest comparable foraminiferal Mg/Ca ratios for *T. sacculifer* at similar temperatures.

359

360 **4.2. Incorporation of Sr into Mg/Ca-Temperature calibrations**

361 Combining Mg and Sr data to compute temperature was first suggested by Reichart et al. (2003)
362 for the aragonitic species *Hoeglundina elegans*. It has been demonstrated that variables other
363 than temperature, such as salinity and carbonate chemistry (possibly via their impact on growth
364 rate) are factors influencing Sr incorporation into calcite (e.g. Lea et al., 1999, Dueñas-
365 Bohórquez et al., 2009; Dissard et al., 2010a; Dissard et al., 2010b). The good correlation of
366 Sr/Ca with temperature in our results ($R^2=0.67$, p value= 5.e-04, Fig 2b), also suggests that
367 temperature exerts a major control on the amount of Sr incorporated into *T. sacculifer*' tests.
368 However, Sr/Ca concentration also shows a correlation with salinity ($R^2=0.29$, p-value=0.053),
369 which is not observed for Mg ($R^2=0.09$, p-value=0.32). Therefore, the incorporation of Sr into
370 the Mg-T reconstruction equation might improve temperature reconstruction by accounting for
371 the impact of salinity. It has recently been suggested that the Sr incorporation in benthic
372 foraminiferal tests is affected by their Mg contents (Mewes et al., 2015; Langer et al.; 2016).
373 However, as pointed out in Mewes et al., (2015), calcite's Mg/Ca needs to be over 30-50mmol
374 in order to noticeably affect Sr partitioning. There is no obvious reason to assume that
375 planktonic foraminifera should have a different Mg/Ca threshold. Therefore, with a
376 concentration between 2 to 6 mmol/mol (Sadekov et al., 2009), the observed variation in Sr
377 concentration in *T. sacculifer*' tests can be safely considered to be independent of the Mg/Ca

378 concentrations. Hence, other environmental parameters such as temperature, salinity and/or
379 carbonate chemistry, potentially via an impact on calcification rates, must control Sr/Ca values.

380

381 The standard deviation of measured temperatures versus reconstructed temperature was
382 calculated for each of the three Mg-temperature equations established in this study. For
383 equation (1), based on Mg/Ca only, SD= 1.37, for equation (3), based on both Mg/Ca and Sr/Ca,
384 SD=0.98, and for equation (4), based on Mg/Ca ratio and salinity, SD=1.03. Incorporation of
385 Sr into the Mg-Temperature reconstruction equation resulted in the standard deviation the
386 closest to 1 (SD=0.98), indicating that this statistically improved reconstructions possibly by
387 attenuating the salinity effect as well as potentially other environmental parameters such as
388 variations in carbonate chemistry or the effect of temperature itself. Therefore, the combination
389 of Mg/Ca and Sr/Ca should be considered to improve temperature reconstructions (Tab. 3). For
390 the remainder of this discussion, and in order to compare our data with previously established
391 calibrations for *T. sacculifer*, the equation based on Mg/Ca alone (equation 1) will be
392 considered.

393

394 **4.3 Comparison with previous *T. sacculifer* Mg/Ca-Temperature calibrations.**

395 Mg/Ca ratios measured on *T. sacculifer* from our study show a strong correlation with measured
396 surface water temperature ($R^2=0.86$, p value= $2.9e-06$) (Fig. 2a), increasing exponentially by
397 8.3% per °C. The relation with temperature (equation 1) is comparable to the one published by
398 Nürnberg et al., (1996) and within the standard error of the calibration (Fig. 3a). This implies
399 that the temperature controlled-Mg incorporation into *T. sacculifer* tests is similar under culture
400 conditions as it is in natural surface waters. The equation established by Duenas-Bohorquez et
401 al., (2010) based on *T. sacculifer* specimen from culture experiments integrates ontogenetic
402 (chamber stage) effects. Even though incorporating the ontogenetic impact may improve
403 temperature reconstructions based on Mg/Ca ratios, this is not routinely done for paleo-
404 temperature reconstruction using *T. sacculifer*. Therefore, the equation of Nürnberg et al.,
405 (1996) is used in our study for comparison of various reconstruction scenarios.

406 A comparable regression (similar slope) has been established for *T. sacculifer* from tropical
407 Atlantic and Caribbean surface sediment samples by Regenberget al. (2009) (Fig 3a). This
408 regression predicts Mg concentrations that are about 0.15 mmol/mol higher compared to our
409 study. Because the Mg-T calibration from Regenberget al. (2009) is based on sediment-surface
410 samples, Mg concentrations were correlated with reconstructed mean annual temperatures. This
411 potentially leads to an over or under-estimation of temperatures depending on the seasonality

412 of the growth period and might explain the observed difference between the two regressions.
413 Due to sample limitation, we analysed foraminifera from a wider size fraction (230µm to
414 500µm), compared to Regenberg et al. (2009) (355-400µm), introducing an additional bias
415 between the two datasets (Duenas-Bohorquez et al., 2010; Friedrich et al., 2012). Finally,
416 Regenberg et al. (2009), compiled data of samples from the tropical Atlantic and Caribbean
417 Ocean, while we collected samples from the Eastern tropical Atlantic. All of these potential
418 biases can easily explain the small discrepancy observed between our regression and the one
419 from Regenberg et al., (2009). Interestingly, Jentzen et al., (2018), were able to compare Mg/Ca
420 ratios measured on *T. sacculifer* from both surface sediment samples of the Caribbean sea and
421 specimen sampled with a plankton net nearby. They observed a similar systematic increased
422 Mg/Ca ratio in fossils tests of *T. sacculifer* (+0.7 mmol/mol-1) compared to living specimens,
423 arguing that different seasonal signals were responsible for the observed difference. However,
424 it is interesting to note that the Mg/Ca differences observed between living *T. sacculifer* (e.g.
425 this study and Jentzen et al., 2018) and fossils specimens (e.g. Regenberg et al., 2009 and
426 Jentzen et al., 2018) could also be explained by the presence of GAM calcite on *T. sacculifer*
427 from sediment samples, as GAM calcite is enriched with Mg compared to pre-gametogenetic
428 calcite precipitated at the same temperature (Nurnberg et al., 1996). If Jentzen et al., (2018) and
429 Regenberg et al. (2009) do not describe the presence or absence of GAM calcite on *T. sacculifer*
430 specimens analysed in their studies, a study on the population dynamics of *T. sacculifer* from
431 the central Red Sea Bijma and Hemleben (1990) concluded that the rate of gametogenesis
432 increased exponentially between 300 and 400µm to reach a maximum of more than 80% at
433 355µm (sieve size =500µm real test length). It can therefore safely be assumed that the Mg/Ca
434 difference between living specimens from the plankton and empty shells from the sediment is
435 due to GAM calcite.

436 The Mg-Temp data obtained by Jentzen et al., (2018) is however, in good agreement with the
437 equation established by Regenberg et al., (2009), and will therefore not be considered separately
438 in this study. The overall strong similarity observed between our regression and the one from
439 Regenberg et al. (2009), indicates nevertheless that Mg-temp calibrations established on *T.*
440 *sacculifer* specimen from plankton tow, can be applied to *T. sacculifer* (without Sac) from the
441 surface-sediment, even if these applications have to be considered with care and only on
442 sediment samples showing no sign of dissolution.

443 In contrast, the equation of Anand et al., (2003) based on sediment trap samples, is appreciably
444 different (Fig. 3b). This may be due to: (1) difference in cleaning and analytical procedures, (2)
445 addition of GAM calcite at greater depth and (3) uncertainty in estimated temperature, indeed,

446 as mentioned in Gray et al., (2019): “Note the calibration line of Dekens et al. (2002) and Anand
447 et al. (2003) does not fit the data of Anand et al. (2003) when climatological temperature, rather
448 than the $\delta^{18}\text{O}_{\text{calcite}} - \delta^{18}\text{O}_{\text{water}}$ temperature, is used. As shown by Gray et al., (2019), we show
449 the calibrations of Anand et al (2003) are inaccurate due to seasonal changes in the $\delta^{18}\text{O}$ of sea
450 water at that site.

451 Anand et al., (2003) fixed the intercept of the exponential regression for *T. sacculifer* to the
452 value obtained for a multispecies regression and subsequently recalculated for each species the
453 pre-exponential coefficients. Using this approach their new equation for *T. sacculifer* is:
454 $\text{Mg}/\text{Ca} = 0.35 \exp(0.09 \cdot T)$, which is identical to Nürnberg et al., (1996) and equation 1 from
455 our study. Still, this implicitly assumes a common temperature dependence exists for all
456 species, which is not realistic. To avoid *a priori* assumptions only the primary equation of
457 Anand et al., (2003) (see Tab. 3) is considered in this study.

458

459 **4.4. Comparison with previous $\delta^{18}\text{O}$ -Temperature calibrations.**

460 As for Mg/Ca, the oxygen isotope composition also shows a strong correlation with measured
461 surface water temperature ($R^2=0.90$). The *T. sacculifer* $\delta^{18}\text{O}$ -temperature equation of Spero et
462 al., (2003), based on a culture experiment, is very similar to equation 4 in our study. However,
463 sensitivity (slope) differs within the uncertainties calculated for equation 4. As no uncertainties
464 are given for the Spero et al., (2003) equation, it is difficult to determine whether these
465 equations are statistically different or not. In contrast, the equation of Mulitza et al., (2003), has
466 a similar slope (within uncertainties) but a higher intercept (Fig. 4a). The equation of Erez and
467 Luz, (1983) differs considerably from equation 4, for both slope and intercept parameters.
468 Bemis et al., (1998) suggested a bias in the calibration due to uncontrolled carbonate chemistry
469 during the experiments of Erez and Luz (1983) (a decrease in pH, e.g. due to bacterial growth
470 in the culture medium or to a higher CO_2 concentration in the lab (air conditioners, numerous
471 people working in the same room etc), would quickly lead to an increase in $\delta^{18}\text{O}$ of culture-
472 grown foraminifera). This could explain the observed effect between our study (equation 4) and
473 the calibration from Erez and Luz (1983). Although the equation of Mulitza et al., (2003) is
474 also based on *T. sacculifer* collected from surface waters, their equation is significantly different
475 from equation (4). This deviation could possibly be due to a difference in size fractions
476 considered in the two studies (230 to 500 μm , and 150 to 700 μm for this study and Mulitza et
477 al., (2003), respectively). Berger et al. (1979), already reported that large *T. sacculifer* tests are
478 enriched in $\delta^{18}\text{O}$ relative to smaller ones (variation of 0.5‰ between 177 and 590 μm).

479 Similarly, in culture experiments, larger shells of *Globigerina bulloides* are isotopically heavier
480 relative to smaller specimens (variation of approximately 0.3‰ between 300 to 415µm,
481 Bemis et al., 1998). Jentzen et al., (2018) reported that: ‘Enrichment of the heavier ¹⁸O isotope
482 in living specimens below the mixed layer and in fossil tests is clearly related to lowered in situ
483 temperatures and gametogenic calcification’. Gametogenic calcite has been shown to enrich
484 δ¹⁸O signatures by about 1.0-1.4‰ relative to pregametogenic *T. sacculifer* (Wyceh et al.,
485 2018). Finally, variation in light intensity (e.g. due to different sampling period and/or sampling
486 location), may have influenced the δ¹⁸O composition via an impact on symbiont activity (Spero
487 and DeNiro, 1987). Bemis et al. (1998) demonstrated that in seawater with ambient [CO₃²⁻],
488 *Orbulina universa* shells grown under high light level (> 380 µEinst m⁻² s⁻¹) are depleted in ¹⁸O
489 by on average 0.33‰ relative to specimens grown under low light levels (20-30 µEinst m⁻² s⁻¹).
490 The different correlation between δ¹⁸O and temperature reported by Mulitza et al., (2003) may
491 be caused by size fraction differences, different sampling time, light intensity, differences in
492 calcification depth or hydrography, or a combination of factors. These are all potential biases
493 that could explain the steeper intercept observed by Mulitza et al., (2003) relative to our study.

494

495 **5. Reconstructions**

496 A few scenarios are considered in the following section, in which one, two or three proxy
497 equations are combined to solve for salinity.

498

499 Three Mg/Ca-paleo-temperature equations (Nürnberg et al., 1996; Regenberg et al., 2009; and
500 Anand et al., 2003) were used to compare “reconstructed” temperatures to the known *in situ*
501 surface waters temperatures. The mean foraminiferal Mg/Ca ratio measured at each of our
502 stations was inserted into each of the three equation and solved for temperature (Fig. 3b.). The
503 linear regression of reconstructed temperatures based on Nürnberg et al. (1996) overlaps almost
504 perfectly with the theoretical best fit. This confirms that calibrations based on culture
505 experiments (the primary geochemical signal recorded in the tests) are very well-suited for
506 reconstructing surface water temperature. The regression from Regenberg et al., (2009)
507 reconstructed surface temperature that are too warm. This is in agreement with the fact that the
508 Mg/Ca ratio from surface sediment foraminifera are slightly higher than for living specimen
509 (Jentzen et al. 2018). The offset increases with decreasing temperature (0.5°C and 1.5°C
510 respectively at 30°C and 16°C). Finally, the reconstructed temperature using the equation from
511 Anand et al. (2003), shows a strong systematic offset. Because the equation of Nürnberg et al.,
512 (1996) matched our measured temperatures almost perfectly, their equation will be used to

513 analyse further reconstruction. Still, we acknowledge that downcore reconstructions will
 514 inevitably also involve GAM calcite and hence other calibrations established using specimens
 515 collected deeper in the water column or in the sediment should be better suitable. Similarly,
 516 three $\delta^{18}\text{O}$ -paleo temperature equations (Erez and Luz, 1983; Mulitza et al., 2003; Spero et al.,
 517 2003) were tested to reconstruct $\delta^{18}\text{Oc}$ - $\delta^{18}\text{Ow}$. The equation of Erez and Luz, (1983), shows a
 518 significant systematic overestimation of $\delta^{18}\text{Oc}$ - $\delta^{18}\text{Ow}$, and will therefore not be considered any
 519 further. Measured surface water temperatures at our 13 stations were inserted into the equations
 520 of Mulitza et al., (2003) and Spero et al., (2003) to derive $\delta^{18}\text{Oc}$ - $\delta^{18}\text{Ow}$ (Fig. 4). The $\delta^{18}\text{Oc}$ -
 521 $\delta^{18}\text{Ow}$ reconstructions based on the equation of Mulitza et al. (2003) and Spero et al. (2003),
 522 are both slightly more positive, than the theoretical best fit. In order to test the robustness of
 523 $\delta^{18}\text{Ow}$ reconstructions from paleoceanographic literature (e.g. Nürnberg and Groeneveld, 2006;
 524 Bahr et al., 2011), we use the reconstructed temperatures based on the Mg/Ca-paleo-
 525 temperature equation from Nürnberg et al., (1996) to predict $\delta^{18}\text{Ow}$ using measured $\delta^{18}\text{Oc}$ and
 526 the equations from Mulitza et al., (2003) and Spero et al. (2003). The reconstructed $\delta^{18}\text{Oc}$ -
 527 $\delta^{18}\text{Ow}$ from inserting the Mg/Ca temperature into these equations is slightly overestimated
 528 (0.5‰), but the offsets remain small enough to consider these as reasonable reconstructions.

529

530 When reconstructing $\delta^{18}\text{Ow}$ by inserting the Mg/Ca temperature and measured $\delta^{18}\text{Oc}$ in both
 531 equations, the correlation coefficients of the linear regressions are weak ($R^2 = 0.19$ and 0.13 for
 532 Spero et al., 2003 and Mulitza et al., 2003, respectively) demonstrating that the reconstructed
 533 $\delta^{18}\text{Ow}$ is not very reliable, therefore no reconstruction of salinity using these equations will be
 534 further tested in this manuscript.

535

536 Nevertheless, to test the robustness of theoretical and empirical salinity reconstructions, we
 537 have the perfect data set at hand, as every parameter is known from *in situ* measurement or
 538 sampling. We will use the equations 1, 4 and 5 established in this study and presented in table
 539 3, for demonstration purposes.

540

$$541 \quad \text{Mg/Ca} = ae^{bT} \quad \text{Eq. 1}$$

542 with $a=0.42(\pm 0.13)$ and $b= 0.083(\pm 0.001)$

543

$$544 \quad T = c + d(\delta^{18}\text{Oc} - \delta^{18}\text{Ow}) \quad \text{Eq. 4}$$

545 with $c=12.08(\pm 1.46)$ and $d=-4.73(\pm 0.51)$

546

547
$$\delta^{18}O_w = eS + f \quad \text{Eq. 5}$$

548 with $e=0.171(\pm 0.04)$ and $f = -4.93(\pm 1.66)$

549 Classically, from those equations it is possible to extract variables estimated from the
550 observation Mg/Ca and $\delta^{18}Oc$ through the equations:

551
$$\hat{T} = \frac{1}{b} (\log (Mg/Ca) - \log(a)) \quad \text{Eq.1'}$$

552
$$\delta^{18}\widehat{O}_w = \delta^{18}Oc - \frac{1}{d} (\hat{T} - c) \quad \text{Eq. 4'}$$

553
$$\hat{S} = \frac{1}{e} (\delta^{18}\widehat{O}_w - f) \quad \text{Eq. 5'}$$

554

555

556 Given that \hat{T} is estimated from the fit from Eq. 1' (fig. 3a) and $\delta^{18}\widehat{O}_w$ is estimated from Eq. 4',
557 \hat{S} is finally calculated from Eq. 5' (figure 5). Hence, the error in \hat{S} is an accumulation of errors
558 from successive fits. In this study the standard deviation of the fit between \hat{S} and the measured
559 salinity for the 13 stations is ± 2.49 and the R^2 is 0.33 (p-value 0.04) (Fig. 6a and b). In
560 conclusion, even the best possible salinity reconstruction based on locally calibrated equations
561 1, 4 and 5 from the present study only allows salinity reconstructions with a precision of ± 2.49 .
562 In the modern Atlantic Ocean, and based on recent sea surface salinity estimation (Vinogradova
563 et al., 2019), such a variability would not allow to distinguish water masses between 60°N to
564 60°S. Similarly, on a temporal timescale, given the regional salinity variations expected in most
565 of the ocean over glacial-interglacial cycles is less than $\pm 1, 2\sigma$ (Gray and Evans, 2019), such an
566 incertitude on salinity reconstruction would not even allow to distinguish modern *versus* last
567 glacial maximum water masses.

568

569 In the following steps, we quantify the error propagation more precisely. In simple cases, error
570 accumulation in an equation can be assessed by calculating the partial derivatives and by
571 propagating the uncertainties of the equation with respect to the predictors (Clifford, 1973).
572 However, for complex functions the calculation of partial derivatives can be tedious. Here, error
573 propagation related to \hat{S} was computed by a Monte Carlo simulation, which is simple to
574 implement (Anderson, 1976), and in line with the method applied by Thirumalai et al., (2019)
575 on sediment samples *G. Ruber* (W) specimen. It is important to note that the propagated error
576 with a reconstructed salinity is a combination of fitting errors and errors associated with
577 measurement inaccuracies (Mg/Ca and $\delta^{18}Oc$). First, we will only consider the error related to
578 the fitting procedure, (Eq. 1', 4' and 5', assuming that variables (i.e. the data) are perfectly

579 known without uncertainties). For example, the fitting error related to Eq. 4' is computed by
 580 fitting $\delta^{18}\text{O}_w$ from measured $\delta^{18}\text{O}_c$ and measured Temperature, i.e. the data are known and
 581 not approximated. This is done by adding random Gaussian noise, with standard deviation
 582 corresponding to the RMSE (Root Mean Square error) of each fit (respectively 1.32°C for
 583 Eq.1', 0.15‰ for Eq. 4' and 0.55 for Eq. 5'). The resulting standard deviation error for the
 584 reconstructed Salinity based on 10000 fits following the Monte-Carlo approach amounted to
 585 ± 1.69 (each fit using sampling from random distributions defined above). Hence, ± 1.69 is the
 586 smallest possible error for salinity reconstructions, using the three steps above, only due to its
 587 mathematics. We can also estimate the error propagation at each step: $\hat{T} \pm 1.32^\circ\text{C}$ (Eq.1'),
 588 $\widehat{\delta^{18}\text{O}_w} \pm 0.45\text{‰}$ (Eq.4') and $\hat{S} \pm 1.69$ (Eq.5'). Now we will include the uncertainties related to
 589 estimating the variables using proxy data. Hereto, some Gaussian noises simulating the
 590 uncertainties of measured variables (Mg/Ca and $\delta^{18}\text{O}_c$) were introduced with standard
 591 deviations taken from Table 2. The resulting standard deviation error increased to ± 2.65 .
 592 Therefore, it can be concluded that statistically speaking, $\widehat{\delta^{18}\text{O}_w}$ cannot be reconstructed to a
 593 precision better than $\pm 0.45\text{‰}$, while salinity cannot be reconstructed to a precision better than
 594 ± 1.69 (fitting errors only) and, in reality hardly better than ± 2.65 (full to error propagation).

595
 596 Finally, to complete this analysis, a direct linear fit to estimate salinity using $\exp(-\delta^{18}\text{O}_c)$
 597 and Mg/Ca was performed and led to an error of ± 0.26 and a $R^2 = 0.82$ (p-value 2.10^{-4}):

$$599 \quad \hat{S} = -0.16(\pm 0.02) e^{-\delta^{18}\text{O}_c} + 0.28(\pm 0.1) \frac{\text{Mg}}{\text{Ca}} + 35.80(\pm 0.33) \quad (R^2=0.81, \text{p-value} \approx 2.10^{-4}) \quad \text{Eq. 6}$$

600
 601 This demonstrates that the direct reconstruction using the exact same variables as those initially
 602 measured (Mg/Ca and $\delta^{18}\text{O}_c$), led to a much better estimation of salinity than the successive
 603 reconstruction.

604
 605
 606 Finally, to complete this analysis, a direct linear fit to estimate salinity using $\exp(-\delta^{18}\text{O}_c)$
 607 and Mg/Ca was performed and led to an error of ± 0.26 and a $R^2 = 0.82$ (p-value 2.10^{-4}):

$$609 \quad \hat{S} = -0.16(\pm 0.02) e^{-\delta^{18}\text{O}_c} + 0.28(\pm 0.1) \frac{\text{Mg}}{\text{Ca}} + 35.80(\pm 0.33) \quad (R^2=0.81, \text{p-value} \approx 2.10^{-4}) \quad \text{Eq. 6}$$

610

611 This demonstrates that the direct reconstruction using the exact same variables as those initially
612 measured (Mg/Ca and $\delta^{18}Oc$), led to a much better estimation of salinity than the successive
613 reconstruction.

614

615

616 **6. Implications**

617 We analyzed shell Mg/Ca and Sr/Ca ratios, and $\delta^{18}O$ in *T. sacculifer* collected from surface
618 water along a North-South transect of the Eastern Tropical Atlantic Ocean. We find a strong
619 correlation between Mg/Ca ratios and surface water temperature, confirming the robustness of
620 surface water temperature reconstructions based on *T. sacculifer* Mg/Ca.

621 Insertion of the Sr/Ca ratio into the paleo-temperature equation improves the temperature
622 reconstruction. We established a new calibration for a paleo-temperature equation based on
623 Mg/Ca and Sr/Ca ratios for live *T. sacculifer* collected from surface water:

624

625

626

627

$$628 \quad T = (-27 \pm 15) + (8 \pm 1) * \ln(\text{Mg/Ca}) + (28 \pm 11) * \text{Sr/Ca}$$

629 Scenarios were tested using previously published reconstructions. Results were compared to
630 reconstructions performed using local calibrations established in this study and therefore
631 supposed to represent the best possible calibration for this data set:

632 (1) Mg/Ca ratios measured in *T. sacculifer* specimens collected in surface water allow accurate
633 reconstruction of surface water temperature.

634 (2) $\delta^{18}Ow$ can be reconstructed with an uncertainty of $\pm 0.45\%$. Such $\delta^{18}Ow$ reconstructions
635 remain a helpful tool for paleo-reconstructions considering the global range of variation of
636 surface $\delta^{18}Ow$ (from about -7 to 2‰, LeGrande and Schmidt 2006;).

637

638 (3) In contrast, the best possible salinity reconstruction based on locally calibrated equations 1,
639 4 and 5 from the present study, only allowed reconstruction with an uncertainty of ± 2.49 . Such
640 an uncertainty renders these reconstructions meaningless and does not allow for viable
641 (paleo)salinity data.

642 This is confirmed by a Monte Carlo simulation, applied to test successive reconstructions in an
643 'ideal case', where explanatory variables are known. This simulation shows that from a pure
644 statistical point of view, successive reconstructions involving Mg/Ca and $\delta^{18}Oc$ preclude

645 salinity reconstruction with a precision better than ± 1.69 and hardly better than ± 2.65 , due to
646 error propagation.

647 Nevertheless, a direct linear fit to reconstruct salinity based on the same measured variables
648 (Mg/Ca and $\delta^{18}O_c$) was established (Eq. 6) and presented in table 3. This direct reconstruction
649 of salinity should lead to a much better estimation of salinity (± 0.26) than the successive
650 reconstructions.

651

652 **ACKNOWLEDGEMENTS**

653 We thank captain and crew of the Polarstern cruise ANT XXIII/1, (Bremerhaven-Cape Town)
654 who have been of great support during this unforgettable experience. We are grateful to Susann
655 Grobe of the Marine Biogeochemistry group of the IFM-GEOMAR (Germany) for measuring
656 DIC and ALK of water samples. We thank Arnold Van Dijk of the Department of Earth
657 Sciences-Geochemistry of the University of Utrecht (The Netherlands) for measuring oxygen
658 isotope composition of water and foraminifera. We are thankful to Gijs Nobbe and Dr. Paul
659 Mason for their support with LA-ICP-MS analyses. We would like to thank Beate Mueller
660 (formaly Hollmann) for her technical support when handling foraminifera, and Dr. Gernot
661 Nehrke, Dr. Stephan Mulitza, and Dr. Aurore Receveur for improving earlier versions of the
662 manuscript. We thank Prof. Dieter Wolf Gladrow for his support during the initial draft of this
663 manuscript. This work was supported by the German research foundation (DFG) under grant
664 no. BI 432/4-2 ("PaleoSalt"), and by the European Science Foundation (ESF) under the
665 EUROCORES Programme EuroCLIMATE through contract No. ERAS-CT-2003-980409 of
666 the European Commission, DG Research, FP6. Gert-Jan Reichart acknowledges funding from
667 the program of the Netherlands Earth System Science Centre (NESSC), by the Ministry of
668 Education, Culture and Science (OCW; Grant 024.002.001).

669

670

REFERENCES

671

- 672 Anand P, Elderfield H, and Conte MH, 2003. Calibration of Mg/Ca thermometry in planktonic
673 foraminifera from a sediment trap time series. *Paleoceanography* 18, 15. DOI:
674 10.1029/2002PA000846.
- 675 Anderson GM, 1976. Error propagation by the Monte Carlo method in geochemical
676 calculations, *Geochimica et Cosmochimica Acta*, Volume 40, Issue 12, 1976, Pages
677 1533-1538. DOI: 10.1016/0016-7037(76)90092-2.

678 Bahr A, Nurnberg D, Schonfeld J, Garde-Schonberg D, 2011. Hydrological variability in
679 Florida Straits during Marine Isotope Stage 5 cold events. *Paleoceanography* 26,
680 PA2214. DOI: 10.1029/2010PA002015.

681 Bé AWH, Spero HJ, and Anderson OR, 1982. The effects of symbiont elimination and
682 reinfection on the life processes of the planktonic foraminifer, *Globigerinoides*
683 *sacculifer*. *Mar. Biol.*, 70: 73-86. DOI: 10.1007/bf00397298.

684 Berger WH, 1979. Stable isotopes in foraminifera In: Lipps JH, Berger WH, Buzas MA,
685 Douglas RG, and Ross CA, Editors, *Foraminiferal Ecology and Paleocology, SEPM*
686 *Short Course vol. 6*, Society of Economic Paleontologists and Mineralogists, Houston,
687 Texas (1979), pp. 56–91. DOI:10.2110/scn.79.06.0156.

688 Bemis BE, Spero HJ, Bijma J, Lea DW, 1998. Reevaluation of the oxygen isotopic composition
689 of planktonic foraminifera: Experimental results and revised paleotemperature
690 equations. *Paleoceanography* 13(2): 150-160. DOI: 10.1029/98PA00070.

691 Bijma J, Faber WW, and Hemleben C, 1990. Temperature and Salinity Limits for Growth and
692 Survival of Some Planktonic Foraminifera in Laboratory Cultures. *Journal of*
693 *Foraminiferal Research* 20, 95-116. DOI: 10.2113/gsjfr.20.2.95.

694 Bijma J and Hemleben C, 1993. Population-dynamics of the planktic foraminifera
695 *Globigerinoides-sacculifer* (Brady) from the central red-sea. *Deep-Sea Research Part*
696 *I-Oceanographic Research Papers* 41: 485-510. DOI: 10.1016/0967-0637(94)90092-2.

697 Bijma J, Hemleben C, and Wellnitz K, 1994. Lunar-Influenced Carbonate Flux of the Planktic
698 Foraminifer *Globigerinoides-Sacculifer* (Brady) from the Central Red-Sea. *Deep-Sea*
699 *Research Part I-Oceanographic Research Papers* 41, 511-530. DOI: 10.1016/0967-
700 0637(94)90093-0.

701 Cleroux C, Cortijo E, Anand P, Labeyrie L, Bassinot F, Caillon N, Duplessy JC, 2008. Mg/Ca
702 and Sr/Ca ratios in planktonic foraminifera: Proxies for upper water column temperature
703 reconstruction. *Paleoceanography* 23. DOI: 10.1029/2007PA001505.

704 Clifford A, 1973. Multivariate error analysis: a handbook of error propagation and calculation
705 in many-parameter systems. *John Wiley and Sons*. ISBN 978-0470160558.

706 Dissard D, Nehrke G, Reichart GJ, Bijma J. 2010a. The impact of salinity on the Mg/Ca and
707 Sr/Ca ratio in the benthic foraminifera *Ammonia tepida*: Results from culture
708 experiments. *Geochimica Et Cosmochimica Acta* 74: 928-940.
709 DOI: 10.1016/j.gca.2009.10.040.

710 Dissard D, Nehrke G, Reichart GJ, Bijma J. 2010b. Impact of seawater pCO₂ on calcification
711 and Mg/Ca and Sr/Ca ratios in benthic foraminifera calcite: results from culturing

712 experiments with *Ammonia tepida*. *Biogeosciences* 7: 81-93. DOI: 10.5194/bg-7-81-
713 2010.

714 Dissard D, Nehrke G, Reichart GJ, Nouet J, Bijma J. 2009. Effect of the fluorescent indicator
715 calcein on Mg and Sr incorporation into foraminiferal calcite. *Geochemistry Geophysics*
716 *Geosystems* 10, Q11001 DOI:10.1029/2009GC002417.

717 Dueñas-Bohórquez A, da Rocha RE, Kuroyanagi A, Bijma J, Reichart GJ. 2009. Effect of
718 salinity and seawater calcite saturation state on Mg and Sr incorporation in cultured
719 planktonic foraminifera. *Marine Micropaleontology* 73: 178-189.
720 DOI: 10.1016/j.marmicro.2009.09.002.

721 Dueñas-Bohórquez A, da Rocha RE, Kuroyanagi A, de Nooijer LJ, Bijma J, Reichart GJ. 2009.
722 Interindividual variability and ontogenetic effects on Mg and Sr incorporation in the
723 planktonic foraminifer *Globigerinoides sacculifer*. *Geochemica and cosmochemica*
724 *acta* 75: 520-532. DOI: 10.1016/j.gca.2010.10.006.

725 Eggins S, De Deckker P, Marshall J. 2003. Mg/Ca variation in planktonic foraminifera tests:
726 implications for reconstructing palaeo-seawater temperature and habitat migration.
727 *Earth and Planetary Science Letters* 212: 291-306. DOI: 10.1016/S0012-
728 821X(03)00283-8.

729 Elderfield H and Ganssen G, 2000. Past temperature and delta O¹⁸ of surface ocean waters
730 inferred from foraminiferal Mg/Ca ratios. *Nature* 405, 442-445. DOI:
731 10.1038/35013033.

732 Emiliani C, 1954. Depth habitats of some species of pelagic foraminifera as indicated by
733 oxygen isotope ratios. *Amer J Sci*, v. 252, p. 149-158. DOI: 10.2475/ajs.252.3.149.

734 Epstein S, Buchsbaum R, Lowenstam HA, and Urey CH, 1953. Revised carbonate-water
735 isotopic temperature scale. *Geological Society of American Bulletin* 64, pp. 1315–1326.
736 DOI: 10.1130/0016-7606(1953)64[1315:RCITS]2.0.CO;2.

737 Erez J, and Luz B. 1983. Experimental Paleotemperature Equation for Planktonic-Foraminifera.
738 *Geochimica Et Cosmochimica Acta* 47, 1025-1031. DOI: 10.1016/0016-
739 7037(83)90232-6.

740 Friedrich O, Schiebel R, Wilson PA, Weldeab S, Beer CJ, Cooper MJ, Fiebig J. 2012. Influence
741 of test size, water depth, and ecology on Mg/Ca, Sr/Ca, δ¹⁸O and δ¹³C in nine modern
742 species of planktic foraminifers. *Earth and Planetary Science Letters* 319-320: 133-
743 145. DOI: 10.1016/j.epsl.2011.12.002.

744 Gaffey SJ and Bronnimann CE, 1993. Effects of Bleaching on Organic and Mineral Phases in
745 Biogenic Carbonates. *Journal of Sedimentary Petrology* 63, 752-754.
746 DOI: 10.1029/2018GC007575.

747 Gray WR, Rae JWB, Wills RCJ, Shevenell AE, Taylor BJ, Burke A, Foster GL; Lear
748 CH (2018): Deglacial planktic foraminiferal boron isotope and Mg/Ca data from
749 sediment core MD01-2416 in the western North Pacific Ocean. *Nature Geoscience*, Vol.
750 11, No. 5, 05.2018, p. 340–344. DOI: 10.1594/PANGAEA.887381.

751 Gray WR and Evans D, 2019. Nonthermal influences on Mg/Ca in planktonic foraminifera: A
752 review of culture studies and application to the last glacial maximum.
753 *Paleoceanography and Paleoclimatology* 34, 306-315. DOI: 10.1029/2018PA003517.

754 Groeneveld J, Ho SL, Mackensen A, Mohtadi M, Laepple T. 2019. Deciphering the variability
755 in Mg/Ca and Oxygen Isotopes of individual foraminifera. *Paleoceanography and*
756 *Paleoclimatology* 34, 755-773. DOI: 10.1029/2018PA003533.

757 Hamilton CP, Spero HJ, Bijma J, Lea DW. 2008. Geochemical investigation of gametogenic
758 calcite addition in the planktonic foraminifera *Orbulina universa*. *Marine*
759 *Micropaleontology* 68: 256-267. DOI: 10.1016/j.marmicro.2008.04.003.

760 Hastings DW, Russell AD, and Emerson SR, 1998. Foraminiferal magnesium in
761 *Globeriginoidea sacculifer* as a paleotemperature proxy. *Paleoceanography* 13, 161-
762 169. DOI: 10.1029/97PA03147.

763 Hemleben C, Spindler M and Anderson OR, 1989. Modern planktonic foraminifera, *Springer*
764 *Verlag, Berlin*, 363 p. ISBN 978-1-4612-3544-6.

765 Honisch B, Allen KA, Lea DW, Spero HJ, Eggins SM, Arbuszewski J, deMenocal P, Rosenthal
766 Y, Russell AD, Elderfield H. 2013. The influence of salinity on Mg/Ca in planktic
767 foraminifera- Evidence from cultures, core-top sediments and complementary $\delta^{18}\text{O}$.
768 *Geochimica et Cosmochimica Acta* 121: 196-213. DOI: 10.1016/j.gca.2013.07.028.

769 Hut G, 1987. Consultant's group meeting on stable isotope reference samples of geochemical
770 and hydrological investigations. *IAEA, Vienna*, p 42 Report to the Director General.
771 INIS-MF—10954.

772 Jentzen A, Nurnberg D, Hathorne EC and Schonfeld J, 2018. Mg/Ca and $\delta^{18}\text{O}$ in living planktic
773 foraminifera from the Caribbean, Gulf of Mexico and Florida Straits. *Biogeosciences*, 15,
774 7077-7095. DOI: 10.5194/bg-15-7077-2018.

775 Jochum KP, Weis U, Stoll B, Kuzmin D, Yang Q, Raczek I, Jacob DE, Stracke A, Birbaum K,
776 Frick DA, Gunther D, Enzweiler J, 2011. Determination of reference values for NIST

777 610-617 glasses following ISO guidelines. *Geostandards and Geoanalytical research*.
778 35, 397–429, 201. DOI: 10.1111/j.1751-908X.2011.00120.x.

779 Johnson KM, Wills KD, Butler DB, Johnson WK and Wong, CS, 1993. Coulometric Total
780 Carbon-Dioxide Analysis for Marine Studies - Maximizing the Performance of an
781 Automated Gas Extraction System and Coulometric Detector. *Marine Chemistry* 44,
782 167-187. DOI: 10.1016/0304-4203(93)90201-X.

783 Kisakurek B, Eisenhauer A, Bohm F, Garbe-Schonberg D, Erez J. 2008. Controls on shell
784 Mg/Ca and Sr/Ca in cultured planktonic foraminiferan, *Globigerinoides ruber* (white).
785 *Earth and Planetary Science Letters* 273: 260-269. DOI: 10.1016/j.epsl.2008.06.026.

786 Kontakiotis G, Mortyn GP, Antonarakou A, Drinia H, 2016. Assessing the reliability of
787 foraminiferal Mg/Ca thermometry by comparing field-samples and culture experiments:
788 a review. *Geological quarterly*, 2016, 60 (3): 547-560. DOI: 10.7306/gq.1272.

789 Langer G, Sadekov A, Thoms S, Keul N, Nehrke G, Mewes A, Greaves M, Misra S, Reichart
790 GJ, de Nooijer LJ, Bijma J, Elderfield H, 2016. Sr partitioning in the benthic
791 foraminifera *Ammonia aomoriensis* and *Amphistegina lessonii*. *Chemical Geology* 440
792 (2016) 306-312. DOI: 10.1016/j.chemgeo.2016.07.018.

793 Lea DW, Mashiotta TA, and Spero HJ, 1999. Controls on magnesium and strontium uptake in
794 planktonic foraminifera determined by live culturing. *Geochimica Et Cosmochimica*
795 *Acta* 63, 2369-2379. DOI: 10.1016/S0016-7037(99)00197-0.

796 Lear CH, Rosenthal Y, and Slowey N, 2002. Benthic foraminiferal Mg/Ca-paleothermometry:
797 A revised core-top calibration. *Geochimica Et Cosmochimica Acta* 66, 3375-3387.
798 DOI: 10.1016/S0016-7037(99)00197-0.

799 LeGrande AN and Schmidt GA, 2006. Global gridded data set of the oxygen isotopic
800 composition in seawater. *Geophys. Res. Lett.* 33, L12604. DOI:
801 10.1029/2006GL026011.

802 Lessa, D., Morard, R., Jonkers, L., Venancio, I. M., Reuter, R., Baumeister, A., Albuquerque,
803 A.L., Kucera, M. (2020). Distribution of planktonic foraminifera in the subtropical
804 South Atlantic: depth hierarchy of controlling factors. *Biogeosciences*, 17(16), 4313-
805 4342. doi:10.5194/bg-17-4313-2020.

806 Mewes A, Langer G, Reichart GJ, de Nooijer LJ, Nehrke G, Bijma J, 2015. The impact of Mg
807 contents on Sr partitioning in benthic foraminifers. *Chemical Geology* 412: 92-98.
808 DOI: 10.1016/j.chemgeo.2015.06.026.

809 Mintrop L, Perez FF, Gonzalez-Davila M, Santana-Casiano MJ, and Kortzinger A, 2000.
810 Alkalinity determination by potentiometry: Intercalibration using three different
811 methods. *Ciencias Marinas* 26, 23-37. DOI: 10.7773/cm.v26i1.573.

812 Mulitza S, Boltovskoy D, Donner B, Meggers H, Paul A, and Wefer G. 2003. Temperature:
813 delta O¹⁸ relationships of planktonic foraminifera collected from surface waters.
814 *Palaeogeography Palaeoclimatology Palaeoecology* 202, 143-152. DOI:
815 10.1016/S0031-0182(03)00633-3.

816 Nürnberg D, Bijma J, and Hemleben C, 1996. Assessing the reliability of magnesium in
817 foraminiferal calcite as a proxy for water mass temperatures. *Geochimica Et*
818 *Cosmochimica Acta* 60, 803-814. DOI: 10.1016/0016-7037(95)00446-7.

819 Nürnberg D and Groenvelde J, 2006. Pleistocene variability of the Subtropical Convergence at
820 East Tasman Plateau: Evidence from planktonic foraminifera Mg/Ca (ODP Site
821 1172A). *Geochem. Geophys. Geosyst.*, 7, Q04P11, DOI:10.1029/2005GC000984.

822 Pahnke K, Zahn R, Elderfield H, Schulz M, 2003. 340,000-Year Centennial-Scale Marine
823 Record of Southern Hemisphere Climatic Oscillation. *Science* 15. Vol. 301, Issue
824 5635, pp. 948-952. DOI: 10.1126/science.1084451.

825 Paul A, Mulitza S, Pätzold J and Wolff T, 1999. Simulation of oxygen isotopes in a global
826 ocean model, from Fisher G, Wefer G. (eds), Use of Proxies in paleoceanography:
827 Examples from the South Atlantic. Springer-Verlag Berlin Heidelberg, pp 655-686.
828 DOI :10.1007/978-3-642-58646-0_27.

829 R Development Core Team (2019). R: A language and environment for statistical computing.
830 R Foundation for Statistical Computing, Vienna, Austria. URL [https://www.R-](https://www.R-project.org/)
831 [project.org/](https://www.R-project.org/).

832 Rathburn AE and DeDeckker P, 1997. Magnesium and strontium compositions of Recent
833 benthic foraminifera from the Coral Sea, Australia and Prydz Bay, Antarctica. *Marine*
834 *Micropaleontology* 32, 231-248. DOI : 10.1016/S0377-8398(97)00028-5

835 Regenberg M, Nürnberg D, Steph S, Groenvelde J, Garbe-Schonberg D, Tiedemann R, Dullo
836 WC, 2006. Assessing the effect of dissolution on planktonic foraminiferal Mg/Ca ratios:
837 Evidence from Caribbean core tops. *Geochemistry Geophysics Geosystems* 7. DOI :
838 10.1029/2005GC001019.

839 Regenberg M, Steph S, Nürnberg D, Tiedemann R, Garbe-Schonberg D, 2009. Calibrating
840 Mg/Ca ratios of multiple planktonic foraminiferal species with delta O¹⁸-calcification
841 temperatures: Paleothermometry for the upper water column. *Earth and Planetary*
842 *Science Letters* 278: 324-336. DOI : 10.1016/j.epsl.2008.12.019.

843 Reichart GJ, Jorissen F, Anschutz P and Mason PRD, 2003. Single foraminiferal test chemistry
844 records the marine environment. *Geology* 31, 355-358. DOI:10.1130/0091-
845 7613(2003)031<0355:SFTCRT>2.0.CO;2.

846 Reynolds RW, NA Rayner, TM Smith, DC Stokes, and W Wang, 2002. An Improved In Situ
847 and Satellite SST Analysis for Climate. *J. Climate*, 15, 1609-1625. DOI:10.1175/1520-
848 0442(2002)

849 Rohling EJ, 2000. Paleosalinity: confidence limits and future applications. *Marine Geology*
850 163, 1-11. DOI: 10.1016/S0025-3227(99)00097-3.

851 Rosenthal Y, Boyle EA and Labeyrie L, 1997. Last glacial maximum paleochemistry and
852 deepwater circulation in the Southern Ocean: Evidence from foraminiferal cadmium.
853 *Paleoceanography* 12, 787-796. DOI: 10.1029/97PA02508.

854 Sadekov A, Eggins SM, De Deckker P, Kroon D, 2008. Uncertainties in seawater thermometry
855 deriving from intratest and intertest Mg/Ca variability in *Globigerinoides ruber*.
856 *Paleoceanography* 23. DOI: 10.1029/2007PA001452.

857 Schmidt GA, 1999. Error analysis of paleosalinity calculations. *Paleoceanography* 14, 422-
858 429. DOI: 10.1029/1999PA900008.

859 Schmidt MW, Spero HJ and Lea DW, 2004. Links between salinity variation in the Caribbean
860 and North Atlantic thermohaline circulation. *Nature* 428, 160-163. DOI:
861 10.1038/nature02346.

862 Shackleton NJ, 1967. Oxygen isotope analyses and Pleistocene temperatures re-assessed,
863 *Nature* 215, 15–17. DOI: 10.1038/21015a0.

864 Shackleton NJ, 1968. Depth of Pelagic Foraminifera and Isotopic Changes in Pleistocene
865 Oceans. *Nature*, 218, 79-80. DOI : 10.1038/218079a0.

866 Shackleton, NJ, 1974. Attainment of isotopic equilibrium between ocean water and the
867 benthonic foraminifera genus *Uvigerina*: isotopic changes in the ocean during the last
868 glacial. *Colloques Internationaux du Centre National du Recherche Scientifique*, 219,
869 203-210. hdl:10013/epic.41396.d001.

870 Spero, H. J., & DeNiro, M. J. (1987). The influence of symbiont photosynthesis on the $\delta^{18}\text{O}$
871 and $\delta^{13}\text{C}$ values of planktonic foraminiferal shell calcite. *Symbiosis*, 4, 213-228.

872 Spero HJ, Mielke KM, Kalve EM, Lea DW and Pak DK, 2003. Multispecies approach to
873 reconstructing eastern equatorial Pacific thermocline hydrography during the past 360
874 kyr. *Paleoceanography* 18. DOI:10.1029/2002PA000814, 2003.

875 Spezzaferri S, Kucera M, Pearson PN, Wade BS, Rappo S, Poole CR, Morard R, Stalder C.
876 2015. *PloS ONE*. 2015; 10 (5): e0128108. DOI: 10.1371/journal.pone.0128108.

877 Thirumalai K, Quinn TM, Marino G 2016. Constraining past seawater $\delta^{18}\text{O}$ and temperature
878 records developed from foraminiferal geochemistry. *Paleoceanography* (2016). DOI:
879 10.1002/2016PA002970

880 Tierney JE, Haywood AM, Feng R, Bhattacharya T, Otto-Bliesner BL (2019): Pliocene SSTs
881 and alkenone saturation indices. *Geophysical Research Letters*, 46, 9136–9144.
882 DOI:10.1594/PANGAEA.904916.

883 Toyofuku T, Kitazato H, Kawahata H, Tsuchiya M, and Nohara M, 2000. Evaluation of Mg/Ca
884 thermometry in foraminifera: Comparison of experimental results and measurements in
885 nature. *Paleoceanography* 15, 456-464. DOI :10.1029/1999PA000460.

886 Vinogradova N, Lee T, Boutin J, Drushka K, Fournier S, Sabia R, Stammer D, Bayler E , Reul
887 N, Gordon A, Melnichenko O, Li LF, Hackert, E, Martin M, Kolodziejczyk N, Hasson
888 A, Brown S ; Misra S; Lindstrom E, 2019. Satellite Salinity Observing System: Recent
889 Discoveries and the Way Forward NASA. *Frontiers in Marine Science*. *Front. Mar. Sci.*
890 6: 243. DOI: 10.3389/fmars.2019.00243.

891 Weldeab S, Schneider RR, Kölling M and Wefer G, 2005. Holocene African droughts relate to
892 eastern equatorial Atlantic cooling. *Geology* 33, 981-984. DOI: 10.1130/G21874.1.

893 Weldeab S, Lea DW, Schneider RR, and Anderson N, 2007. 155,00 years of west African
894 monsoon and ocean thermal evolution. *Science* 316, 130301307.
895 DOI:10.1126/science.1140461.

896 Wyceh JB, Clay Kelly D, Kitajima K, Kozdon R, Orland IJ, Valley JW. 2018. Combined effects
897 of gametogenic calcification and dissolution on $\delta^{18}\text{O}$ measurements of the planktic
898 foraminifer *Trilobatus sacculifer*. *Geochemistry Geophysics Geosystems* 19, 4487-
899 4501. DOI :10.1029/2018GC007908.

900
901
902
903
904
905
906
907
908

909
 910
 911
 912
 913
 914
 915
 916
 917
 918
 919
 920

Table 1. Measured temperature, salinity, DIC, ALK, and $\delta^{18}\text{O}_w$ of the stations selected for this study (October/November 2005).

Stations	Latitude	Longitude	Measured T°C (±0.05) Oct/Nov.	Salinity (±0.05)	DIC (μmol/kg) precision 1μm/Kg accuracy 2 μm/Kg	Alkalinity (μmol/kg) precision 1.5 μm/Kg accuracy 4 μm/Kg	$\delta^{18}\text{O}_w$ (PDB) precision 0.1 ‰ accuracy 0.2 ‰
25	22°38.640'N	20°23.578'W	24.91	36.63	2069	2391	1.1
29	18°8.088'N	20°55.851'W	26.09	36.24	2037	2369	0.9
31	14°32.128'N	20°57.251'W	28.24	35.78	2009	2330	0.8
35	10°23.424'N	20°4.869'W	29.73	35.63	1982	2304	1.2
38	7°2.114'N	17°27.818'W	29.43	34.67	1929	2257	0.7
40	4°22.323'N	15°16.911'W	28.47	34.35	1915	2214	0.8
42	2°15.702'N	13°33.854'W	27.56	35.72	2002	2332	1.1
46	1°35.741'S	10°33.846'W	25.91	36.13	2053	2346	1.0
49	4°44.752'S	8°6.641'W	24.59	36.07	2057	2369	0.9
52	8°6.086'S	5°29.077'W	23.80	35.99	2062	2360	0.7
56	11°51.783'S	2°30.743'W	22.18	36.38	2071	2387	1.0
62	17°59.620'S	2°25.321'E	19.11	35.99	2100	2369	1.1
66	22°26.998'S	6°6.922'E	18.71	35.68	2070	2349	1.0

921
 922
 923
 924
 925
 926
 927
 928
 929

930
 931
 932
 933
 934
 935
 936
 937
 938 **Table 2.** Mean elemental (Mg/Ca and Sr/Ca) and isotopic ($\delta^{18}\text{Oc}$) composition per station, measured
 939 in foraminiferal calcite in mmol/mol and ‰ PDB, respectively. Elemental and isotopic compositions
 940 were determined on the same material (n varying from 5 to 13 specimens per station); isotopic analyses
 941 were done in duplicate for each station. Mean $\delta^{18}\text{Oc}$ - $\delta^{18}\text{Ow}$ measured per stations in ‰ PDB.
 942

Stations	Measured Mg/Ca mmol/mol	Measured Sr/Ca mmol/mol	Measured $\delta^{18}\text{Oc}$ ‰ (V-PDB) precision 0.08‰	Measured $\delta^{18}\text{Oc}$ - $\delta^{18}\text{Ow}$ ‰ (V-PDB)	Recons. $\delta^{18}\text{Ow}$ (Mulitza) ‰ (V-PDB)	Recons. $\delta^{18}\text{Ow}$ (Spero) ‰ (V-PDB)	Recons. $\delta^{18}\text{Ow}$ (this study) ‰ (V-PDB)
25	3.22 ± 0.51	1.53 ± 0.08	-1.76	-2.82	0.38	0.40	0.88
29	4.01 ± 0.24	1.52 ± 0.06	-1.75	-2.63	1.00	0.87	1.44
31	4.78 ± 0.37	1.56 ± 0.18	-2.51	-3.33	0.73	0.49	1.11
35	5.46 ± 0.38	1.59 ± 0.08	-2.35	-3.59	1.27	0.94	1.62
38	4.31 ± 1.14	1.58 ± 0.14	-2.89	-3.59	0.07	-0.10	0.49
40	4.07 ± 0.64	1.57 ± 0.07	-2.98	-3.78	-0.18	-0.32	0.25
42	3.79 ± 0.49	1.53 ± 0.08	-2.38	-3.44	0.21	0.12	0.67
46	3.92 ± 1.24	1.47 ± 0.07	-1.67	-2.66	1.02	0.91	1.46
49	2.99 ± 0.39	1.55 ± 0.11	-1.83	-2.74	0.10	0.16	0.62
52	2.97 ± 0.30	1.50 ± 0.03	-1.34	-2.08	0.57	0.64	1.09
56	3.31 ± 0.53	1.50 ± 0.03	-1.06	-2.10	1.15	1.15	1.65
62	2.20 ± 0.24	1.47 ± 0.07	-0.70	-1.76	0.38	0.64	0.99
66	1.66 ± 0.17	1.48 ± 0.09	-0.74	-1.75	-0.46	-0.02	0.23

943
 944
 945
 946
 947

948
 949
 950
 951
 952
 953
 954

Table 3. Calibration equations for *T. sacculifer*.

Source			R ²	p-values
Mg/Ca Relationship with Temperature				
This study	Mg/Ca=0.42(±0.13)e^{(T*0.083(±0.001))}	Eq. 1	0.86	2.9e-06
Nürnberg et al., 1996	Mg/Ca=0.37(±0.065)e ^{(T*0.091(±0.007))}		0.93	
Anand et al., 2003	Mg/Ca=1.06(±0.021)e ^{(T*0.048(±0.012))}			
Regenberg et al., 2009	Mg/Ca=0.6(±0.16)e ^{(T*0.075(±0.006))}			
Sr/Ca Relationship with Temperature				
This study	Sr/Ca=(0.0094±0.002)*T+(1.29 ± 0.05)	Eq. 2	0.67	5.e-04
Mg/Ca and Sr/Ca Relationship with Temperature				
This study	T=(-27±15)+(8±1)*ln(Mg/Ca)+(28±11)*Sr/Ca	Eq. 3	0.93	2 e-04
Me/Ca Relationship with Temperature and Salinity				
This study (Mg/Ca)	Mg/Ca=exp((-5.10±2)+(0.09±0.009)*T+(0.11±0.05)*S)		0.91	5.e-06
This study (Sr/Ca)	Sr/Ca = (1.81±0.5) + (0.008±0.002) T - (0.01±0.01)*S		0.71	0.002
δ¹⁸O Relationship with Temperature				
This study	T= 12.08(±1.46)-4.73(±0.51)*(δ¹⁸O_c -δ¹⁸O_w)	Eq. 4	0.88	1.6 e-06
Erez and Luz, (1983)	T= 16.06(±0.549)-5.08(±0.32)*(δ ¹⁸ O _c -δ ¹⁸ O _w)			
Mulitza et al., (2003)	T= 15.35(±0.71)-4.22(±0.25)*(δ ¹⁸ O _c -δ ¹⁸ O _w)			
Spero et al., (2003)	T= 12-5.67*(δ ¹⁸ O _c -δ ¹⁸ O _w)			
measured δ¹⁸O vs. measured Salinity (this study)	δ¹⁸O_w = (0.171±0.04)*S - (4.93 ±1.66)	Eq. 5	0.38	1.2 e-03
direct linear fit to reconstruct salinity based on measured variables (Mg/Ca and δ¹⁸O_c)	S = -0.16 (±0.02) e^(- δ¹⁸O_c)+ 0.28 (±0.1) Mg/Ca+35.80 (±0.33)	Eq. 6	0.82	< 2e-04

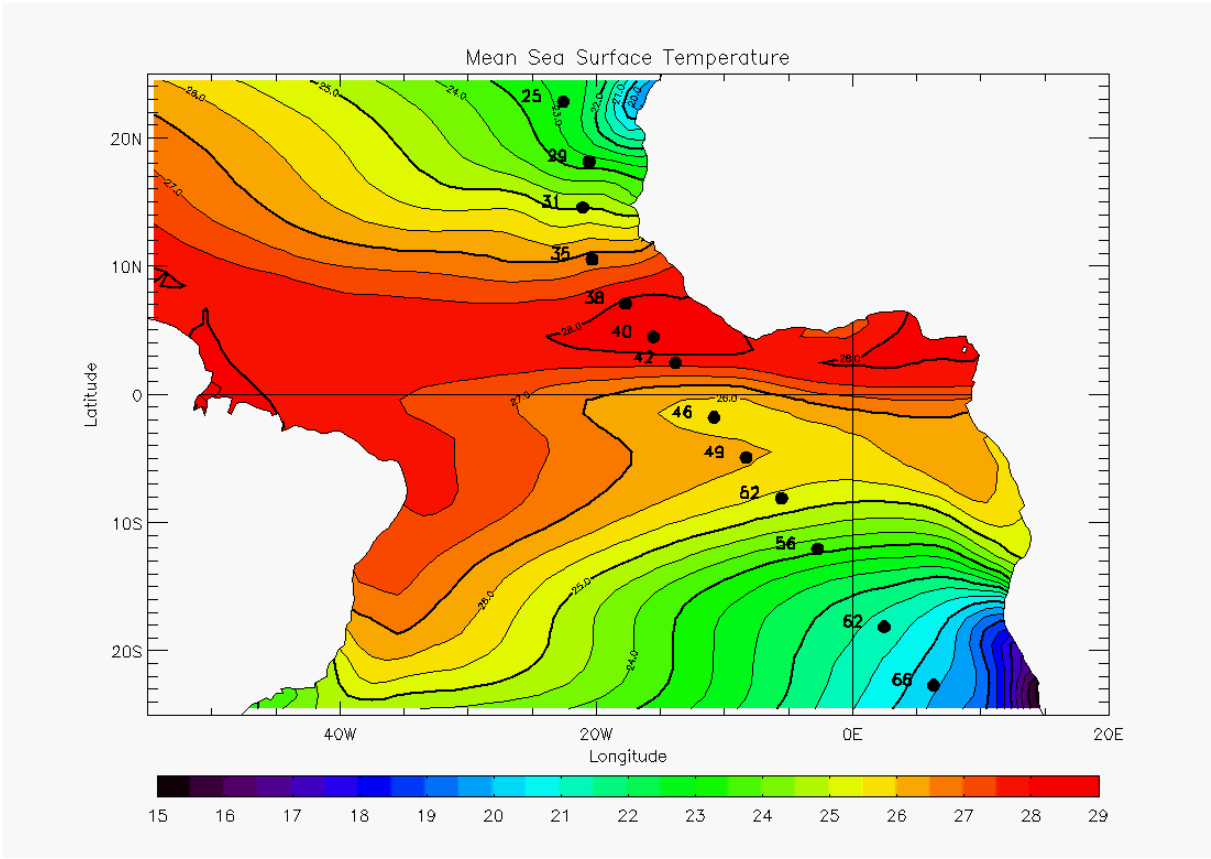
955
 956
 957
 958
 959
 960
 961
 962

963
 964
 965
 966
 967
 968
 969

Table 4. Temperature, salinity and $\delta^{18}\text{O}_w$ of the stations used to determine the salinity/ $\delta^{18}\text{O}_w$ relationship (equation 5)

Stations	Latitude	Longitude	T°C(±0.05)	Salinity(±0.05)	$\delta^{18}\text{O}_w$ (SMOW) precision 0.1% accuracy 0.2%
19	33°20.14'N	14°38.45'W	22.09	36.83	1.3
21	30°23.42'N	16°24.99'W	23.01	36.91	1.4
23	25°20.68'N	18°4.17'W	24.87	37.01	1.8
25	22°38.64'N	20°23.58'W	24.91	36.63	1.3
29	18°8.09'N	20°55.85'W	26.09	36.24	1.1
31	14°32.13'N	20°57.25'W	28.24	35.78	1.1
35	10°23.424'N	20°4.869'W	29.73	35.63	1.5
36	9°5.71'N	19°14.21'W	29.29	35.63	1.1
37	7°43.88'N	18°5.42'W	29.25	34.92	1.0
38	7°2.11'N	17°27.82'W	29.43	34.67	1.0
39	5°49.51'N	16°29.68'W	29.34	34.34	1.0
40	4°22.32'N	15°16.91'W	28.47	34.35	1.1
42	2°15.70'N	13°33.85'W	27.56	35.72	1.3
43	0°57.53'N	12°33.06'W	26.48	36.05	1.3
46	1°35.74'S	10°33.85'W	25.91	36.13	1.3
47	2°17.53'S	10°1.35'W	26.16	36.2	1.2
49	4°44.75'S	8°6.64'W	24.59	36.07	1.2
51	6°55.67'S	6°24.31'W	24.28	36.01	1.1
52	8°6.09'S	5°29.08'W	23.8	35.99	1.0
56	11°51.79'S	2°30.74'W	22.18	36.38	1.3
62	17°59.62'S	2°25.32'E	19.11	35.99	1.3
66	22°26.99'S	6°6.92'E	18.71	35.68	1.3
69	25°0.20'S	8°17.16'E	18.19	35.64	0.9
72	27°2.39'S	10°35.53'E	18.5	35.64	1.0

970
 971
 972
 973
 974



975
 976
 977
 978

Figure 1a

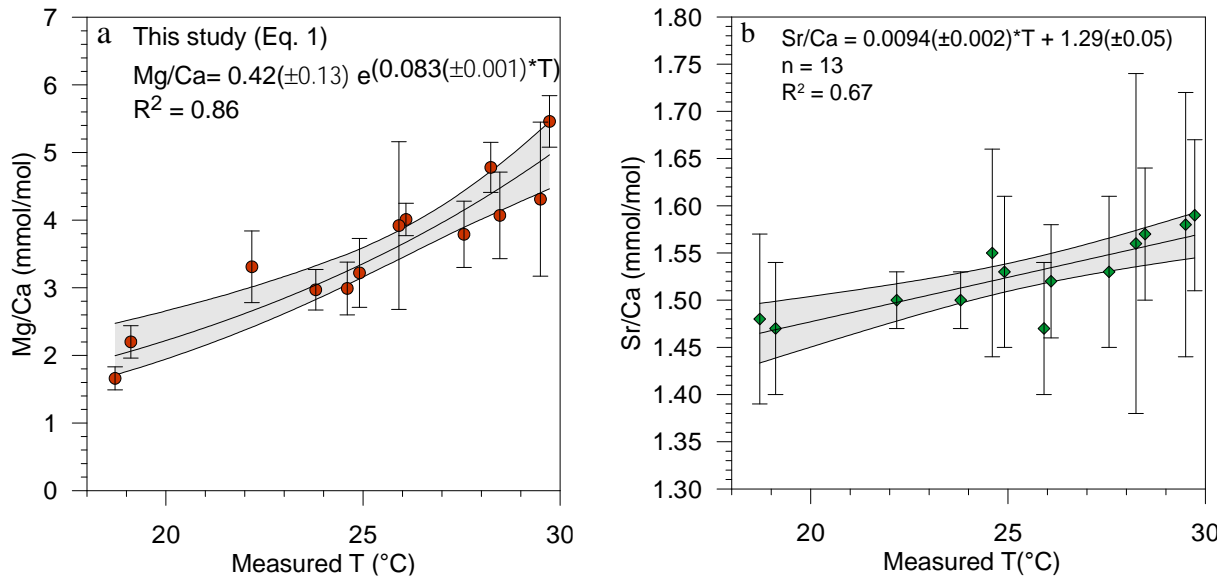


979
 980
 981
 982
 983

Figure 1b

984

985



986

987

988

989

990

991

992

993

994

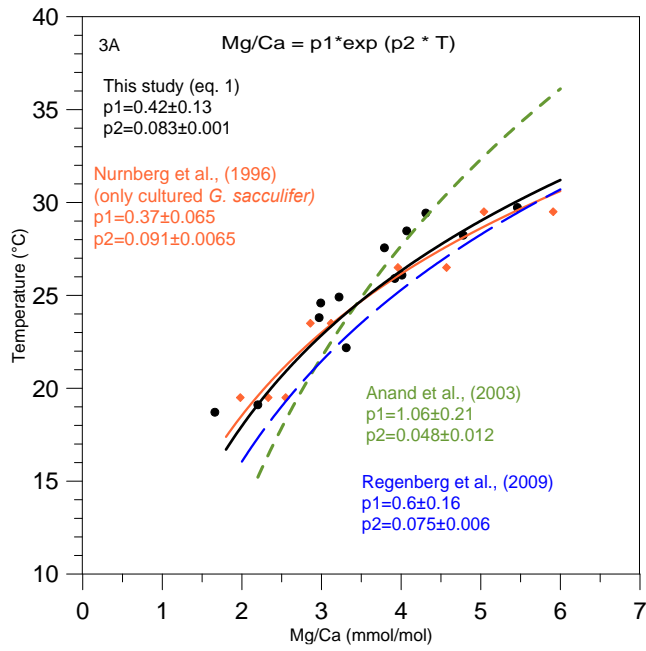
995

996

997

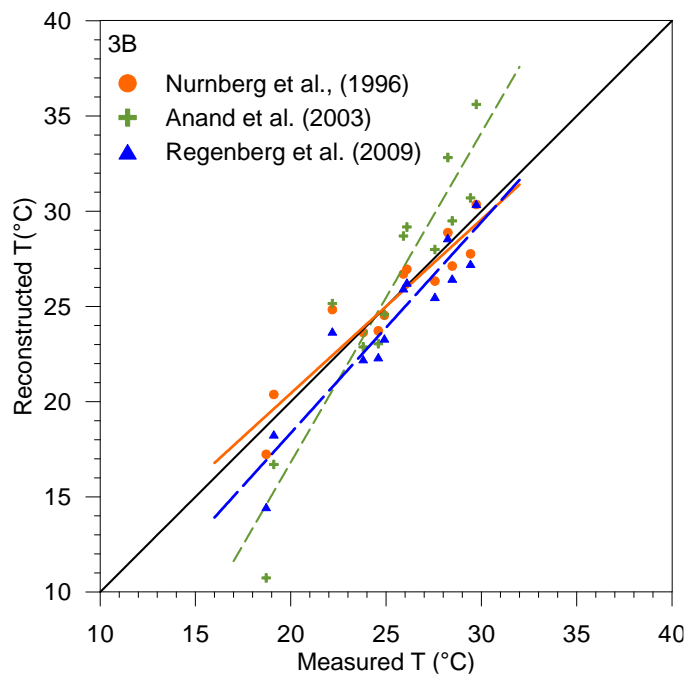
998

Figure 2



999

1000



1001

1002

1003

1004

1005

1006

1007

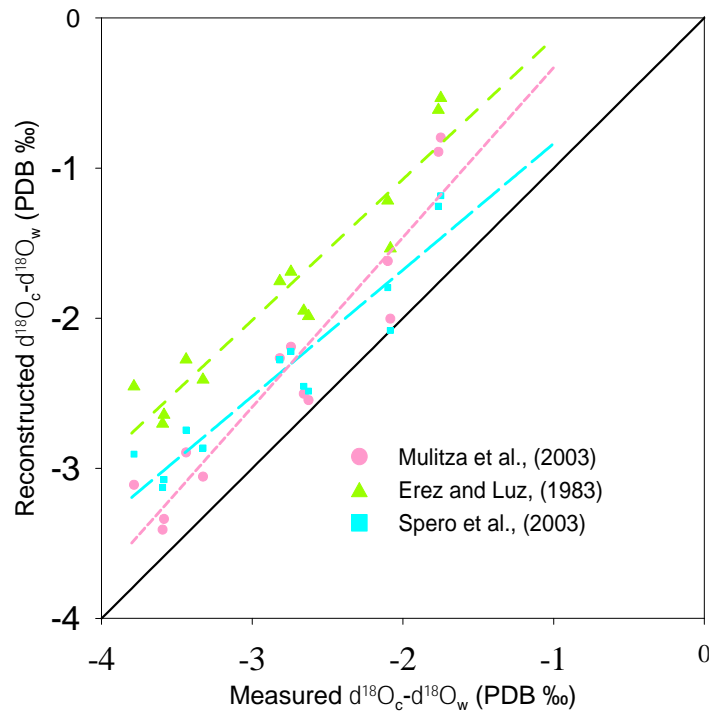
1008

1009

Figure 3

1010

1011



1012

1013

1014

1015

1016

1017

1018

1019

1020

1021

1022

1023

1024

Figure 4

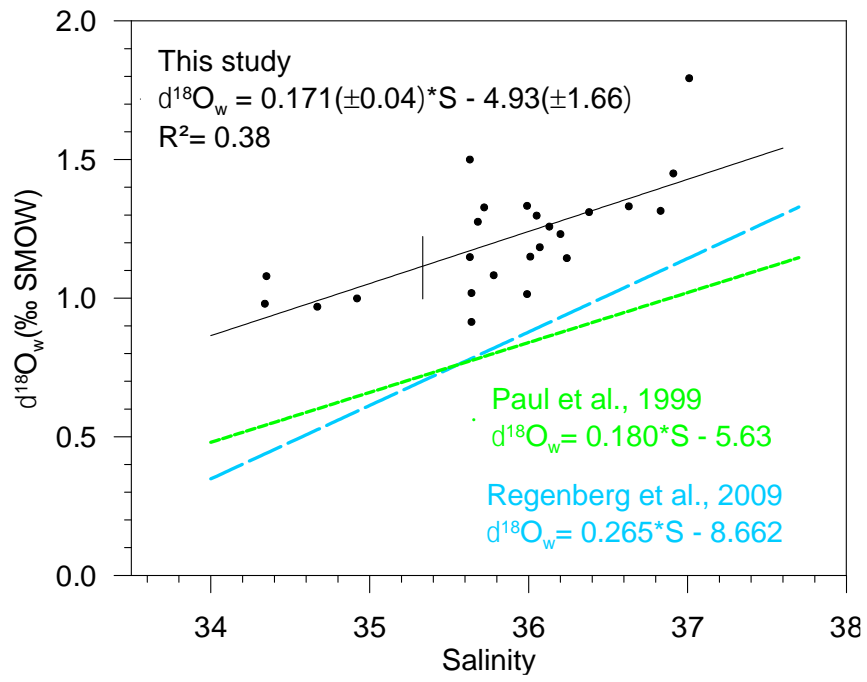
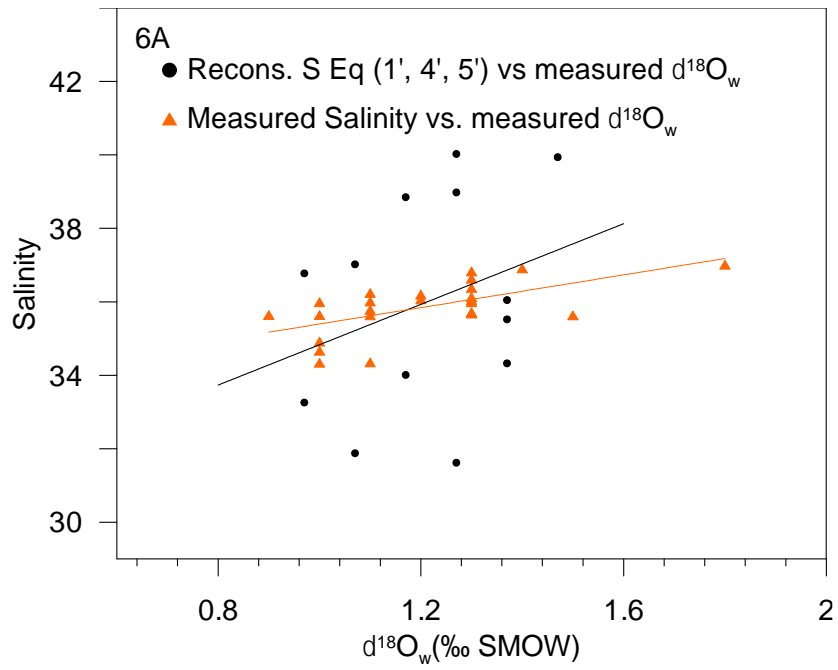


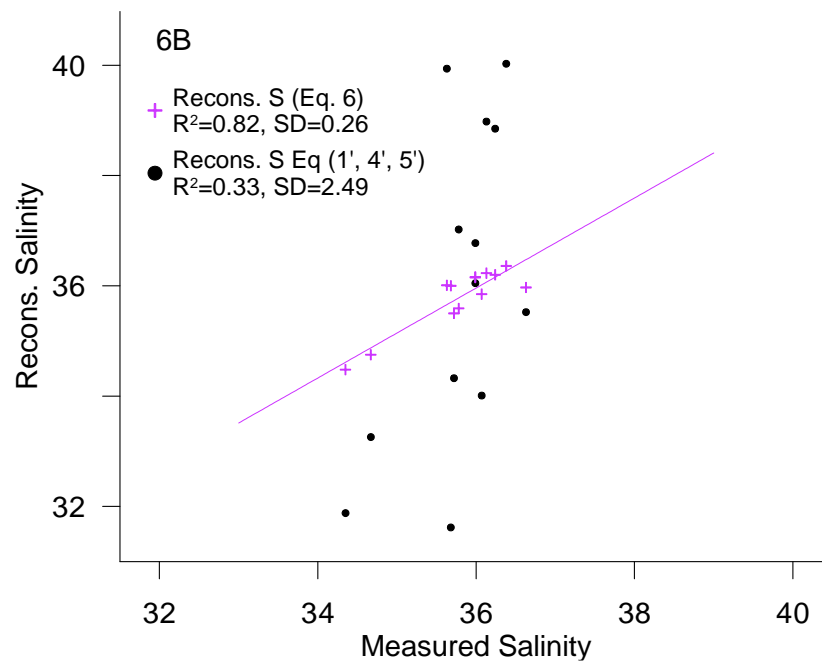
Figure 5

1025
 1026
 1027
 1028
 1029
 1030
 1031
 1032
 1033
 1034
 1035
 1036
 1037
 1038
 1039
 1040
 1041
 1042
 1043
 1044



1045

1046



1047

1048

1049

1050

1051

1052

1053

1054

1055

Figure 6

FIGURE LEGENDS

1056

1057

1058 **Fig. 1:** Stations used in this study, plotted on gridded data set Reynolds et al., (2002) (a). Set
1059 up for planktonic foraminifera collections (b).

1060

1061 **Fig. 2:** (a) Mg/Ca and (b) Sr/Ca (mmol/mol) and 95% confidence intervals plotted versus
1062 measured surface temperature (°C). Each point represents an average of the Mg/Ca and Sr/Ca
1063 per station.

1064

1065 **Fig. 3 a)** Mg/Paleo-temperature equations established in this study (equation 1) (black dots, and
1066 full lines), based on the data of Nürnberg et al., (1996) (Orange diamond and large full orange
1067 line); Anand et al., (2003) (small green dotted line) and Regenberg et al., (2009) (large blue
1068 dotted line) and **3b)** Reconstructed Mg-temperatures (Oct/Nov. 2005) plotted versus measured
1069 temperatures (°C) presented in Table 1. For each station mean measured Mg/Ca was inserted
1070 into the equation of Nürnberg et al., (1996) (only cultured specimens of *T. sacculifer*) (orange
1071 dots, full line), the equation of Anand et al., (2003) (green crosses, small dashed line), and the
1072 equation of Regenberg et al., (2009) (blue triangles, large dashed lines).

1073

1074 **Fig. 4:** Reconstruction of $\delta^{18}\text{Oc}-\delta^{18}\text{Ow}$ by inserting the measured temperature into three $\delta^{18}\text{O}$
1075 based paleo-T-equation: The equation of Spero et al., (2003) (light blue squares, large light blue
1076 dashed line), the equation of Mulitza et al., (2003) (pink dots, small pink dashed line), the
1077 equation sorted by Erez and Luz (1983) (green triangles, green dashed line) plotted versus
1078 measured $\delta^{18}\text{Oc}-\delta^{18}\text{Ow}$ (‰ PDB). The diagonal line represents the 1:1 regression.

1079

1080 **Fig. 5:** Measured surface $\delta^{18}\text{Ow}$ (‰ SMOW) plotted versus measured surface salinity (stations
1081 listed in Tab. 4) (black dots and full line). Regression lines of the $\delta^{18}\text{Ow}$ -salinity relationship
1082 calculated by Paul et al., (1999) for the tropical Atlantic Ocean (from 25°S to 25°N) based on
1083 GEOSECS data (green line), and by Regenberg et al., (2009) (blue dashed line) based on
1084 Schmidt (1999) data for the Atlantic Ocean for the water depth interval of 0–100 m.

1085

1086 **Fig. 6:** a) Measured salinity (orange triangles) and reconstructed salinity based on equations 1,
1087 4 and 5 from the present study (black dots), plotted versus measured $\delta^{18}\text{Ow}$.

1088 b) Reconstructed salinity based on 1) successive reconstructions using equations 1, 4 and 5
1089 from the present study (black dots) and 2) direct linear fit (Eq. 6) based on the same measured
1090 variables (Mg/Ca and $\delta^{18}Oc$) (purple crosses), plotted versus measured salinity.

1091

1092

1093

1094

1095

1096